Earth Systems, Resources, and Sustainability, 2026, 1(1), 44–71

Scilight

Earth Systems, Resources, and Sustainability

Journal Homepage: https://www.sciltp.com/journals/esrs

Article

Volcanic Hazards in an Evolving Earth: Monitoring Magmatic Systems, External Forcing and Beyond

Sambit Sahoo* and Bhaskar Kundu

Department of Earth & Atmospheric Sciences, NIT Rourkela, Rourkela 769008, India

* Correspondence: sambits2009@gmail.com

ABSTRACT

The Earth has evolved dynamically since its formation about 4.5 billion years ago, driven by continuous internal and surface processes. Magmatic systems, driven by Earth's internal heat engine, have evolved from widespread primordial magmatism during early crustal formation to complex, localized activities associated with plate tectonics, mantle plumes, and subduction zones. Volcanoes and hydrothermal systems provide valuable insights into Earth's magmatic processes, which often result in crustal deformations due to the injection, accumulation, and movement of magmatic fluids. Depending on complex physical conditions, these processes can be further influenced by various external and dynamic factors. Exogenous processes do not affect the general trend of magmatic inflation and the rate of increase in magma injection or accumulation, but rather modulate the driving factors. The interplay between endogenous forces (such as magmatic activity) and exogenous factors (such as tectonic stresses or atmospheric phenomena) complicates the understanding and prediction of hazards. The hazards associated with magmatic systems have increased worldwide as communities increasingly settle near these systems to capitalise on their economic and environmental benefits while also disrupting the natural processes through artificial impact. Such regions include the Cascades, the Nordic countries, the Southern Alps, Southeast Asia, and numerous volcanic islands. Under the current scenario of climate change and changing weather patterns, this further complicates the intricate feedback response between endogenous and exogenous forces. This review offers a novel synthesis of the interplay between endogenous and exogenous processes governing magmatic systems, highlighting how external forces modulate volcanic and hydrothermal activity across spatial and temporal scales. We propose a conceptual framework linking external stress perturbations with internal magma dynamics, emphasizing feedback mechanisms during different stages of the eruption cycle. By integrating multi-source geophysical, geodetic, and climatic observations, the study identifies knowledge gaps in understanding how natural forcing affects magmatic inflation, deformation, and eruption forecasting. Under the current scenario of global climate change and increasing anthropogenic impacts, such an integrated perspective is essential for advancing next-generation volcanic monitoring and hazard mitigation strategies.

ARTICLE INFO

History:

Received 17 October 2025
Revised 12 November 2025
Accepted 19 November 2025
Published: 24 November 2025

Keywords:

magmatic systems;
volcanic hazards;
climate change;
volcano monitoring;
caldera dynamics;
fluid flow;
triggering and modulation

Citation:

Sahoo S.; Kundu B. Volcanic Hazards in an Evolving Earth: Monitoring Magmatic Systems, External Forcing and Beyond. *Earth Systems, Resources, and Sustainability* **2026**, *1*(1), 44–71.

Research Highlights

- Volcanoes and hydrothermal systems provide valuable insights into Earth's magmatic processes.
- Climate change and changing weather patterns exert significant control over feedback response between endogenous and exogenous forces.
- Call for integrated perspective for advancing next-generation volcanic monitoring and hazard mitigation strategies.

1. Introduction

Volcanic and hydrothermal systems around plate boundaries and in intra-plate regions are the major magmatic systems associated with mantle convection, where hot magmatic fluids reach the surface through eruptions and fluid migration. Upon reaching, the cooling of the magmatic fluids can form precious ore deposits and fertile soils through subsequent eruptions and hydrothermal circulations. For thousands of years, the economic value of ore deposits and the high fertility of soils produced by successive volcanic eruptions around active volcanoes have consistently drawn human settlements. Additionally, the rich mineral deposits and diverse bio-community surrounding the hydrothermal systems, along with natural renewable energy sources and significant tourism potential, have consistently attracted human habitation in the vicinity of the active systems. The current scenario of climate change and induced phenomena from several artificial activities are proven to be affecting the magma transport and eruptive episodes in the magmatic systems. They could be directly impacted by potential eruptions and unrest episodes. Currently, more than 800 million people reside near active volcanoes and hydrothermal systems globally. They could be directly affected by potential eruptions and unrest episodes, which can cause surface deformation and seismic events [1].

Eruptions are caused by a combination of endogenous processes that begin with the generation and supply of melt from the mantle, followed by magma accumulation in crustal reservoirs and magma transport from storage reservoirs to the surface [1, 2]. Naturally, a volcanic eruption is a phenomenon that requires large volumes of magma with low viscosity, the accumulation of sufficient pressure, a suitable conduit system, and many other satisfying pre-requisites, which in themselves are extremely limited [3]. Furthermore, in the case of hydrothermal systems, the fluids follow migration pathways that depend on the permeability structure of the medium to interact with the host rocks and generate fissures through fractures [4, 5]. Although the fluids follow complex pathways and dynamics to reach the surface and are hard to detect, the numbers reach 100 active volcanoes each year and over 10 erupt simultaneously worldwide [6]. Therefore, accurate forecasting, measurement, and interpretation of volcanic processes are vital for global safety.

Additionally, magmatic systems are considered complex systems that evolve spatiotemporally, driven by their internal dynamics. Depending upon the internal dynamics and fluid pathway conditions the eruption patterns and the lithospheric deformations may vary accordingly. These systems have long been observed to exhibit (pseudo) cycles across different timescales where regional tectonics and earthquakes play a critical role by altering the stress state at volcanoes. These cycles are detected on shorter timescales through seismic activity, degassing patterns, and variations in eruptive frequency and intensity. On longer timescales, they are evident in changes to eruption rates or eruptive flux.

Furthermore, the presence of shallow hydrothermal reservoirs renders the systems susceptible to near-surface natural processes. Therefore, volcanic activities are neatly explored as a culmination of complex interactions between internal processes and external influences, occurring across varying spatial and temporal scales [7–10] (Figure 1). Advances in technology and data processing methods have significantly improved the ability to identify these periodic signals within volcanological datasets. This has revealed the influence of exogenous factors, such as Earth tides and seasonal hydrological variations, as well as climate-driven modulations that act through changes in pore-fluid pressure or the stress field (both dynamic and static). Furthermore, climate change manifests as changes in patterns of temperature, rainfall, snow cover, oceanic currents, etc. also impart sufficient external stress perturbations to disrupt the internal process and modulate the systematic processes. This can influence the dynamics of an active magmatic system, and in some cases, they may serve as the ultimate triggers for volcanic eruptions [11, 12]. Understanding the interactions between internal and external processes at various scales in magmatic systems is crucial for revealing the factors that influence magma ascent, flow, storage, and the conditions leading to volcanic unrest, failure, and eruption triggers. By unraveling the temporal evolution of volcanic activity across both short and long timescales, we can enhance our ability to interpret volcanic histories, assess hazards, and ultimately improve forecasting accuracy and reliability.

In this review article, we have explored the hazards associated with the magmatic system in the context of an evolving Earth where the dynamics keep getting changed over time. Section 2 discusses the societal significance of magmatic systems and summarizes documented hazards, advances in monitoring, and the internal dynamics of magma chambers, caldera cycles, and eruption mechanisms. Section 3 presents a chronological overview of the scientific advancements in monitoring magmatic systems and quantifying external forcing. Section 4 synthesizes key insights and identifies unresolved challenges, focusing on how exogenous forces such as rainfall, tidal loading, and climate variability modulate magmatic processes. Finally, Section 5 outlines future research perspectives and directions for improving volcano monitoring and hazard mitigation in the framework of coupled internal–external Earth processes.

2. Significance of the Magmatic Systems to the Society and Knowledge Advancements

2.1. Documented Hazards Associated with the Magmatic Systems and Advancements in Monitoring and Mitigation

Volcanic eruptions have caused significant fatalities throughout history due to hazards such as pyroclastic flows, lahars, tsunamis, and ashfall, as well as indirect effects like famine (Figures 2 and 3). The notable well-documented examples include the 1815 Mount Tambora eruption in Indonesia that killed about 71,000 people, with

many dying from famine caused by the "Year Without a Summer." Similarly, the 1883 eruption of Krakatoa resulted in over 36,000 deaths, primarily due to tsunamis that devastated coastal areas. Pyroclastic flows are particularly deadly, as seen in the 1902 eruption of Mount Pelée in Martinique, which destroyed Saint-Pierre and killed nearly 29,000 people. Lahars, or volcanic mudflows, caused around 23,000 deaths during the 1985 eruption of Nevado del Ruiz in Colombia when they buried the town of Armero. Tsunamis linked to eruptions, like those triggered by the 1792 eruption of Mount Unzen in Japan, have also been devastating, killing 15,000 people. Ashfall can lead to long-term impacts, such as during the 1783 Laki eruption in Iceland, which caused about 10,000 deaths from fluorine poisoning and famine. Even modern eruptions, like Mount St. Helens in 1980, which killed 57 people, and the Soufrière Hills eruption in Montserrat, which caused 19 deaths, demonstrate the persistent threat of volcanic activity. In addition, eruption-related atmospheric hazards have also been studied, and they can significantly influence weather and climatic patterns.

The outgassing of hazardous gases (SO_2, HCl, and HF) can affect the livestock and negatively impact the population's health and well-being, which is a good example of the effects of prolonged eruptive activity on society. Volcanic dust and ash in the upper troposphere pose a significant threat to air travel, as they can cause damage to static tubes and turbine blades, leading to engine failures that adversely affect air traffic (Figure 3). As a recent example, the 2022 Hunga Tonga-Hunga Ha'apai eruption was a powerful volcanic event in the South Pacific on 15 January 2022 (Figure 3h). Although being a sub-marine volcano, the direct impact of hazards was limited, but the event triggered tsunamis that impacted Tonga, Fiji, and distant nations, with ash fall contaminating water supplies and damaging crops. The eruption sent a massive plume over 58 km high, disrupting global weather and releasing record water vapor into the atmosphere. Tonga experienced major communication outages due to damage to undersea cables. With energy comparable to hundreds of atomic bombs, the eruption had far-reaching environmental and atmospheric effects.

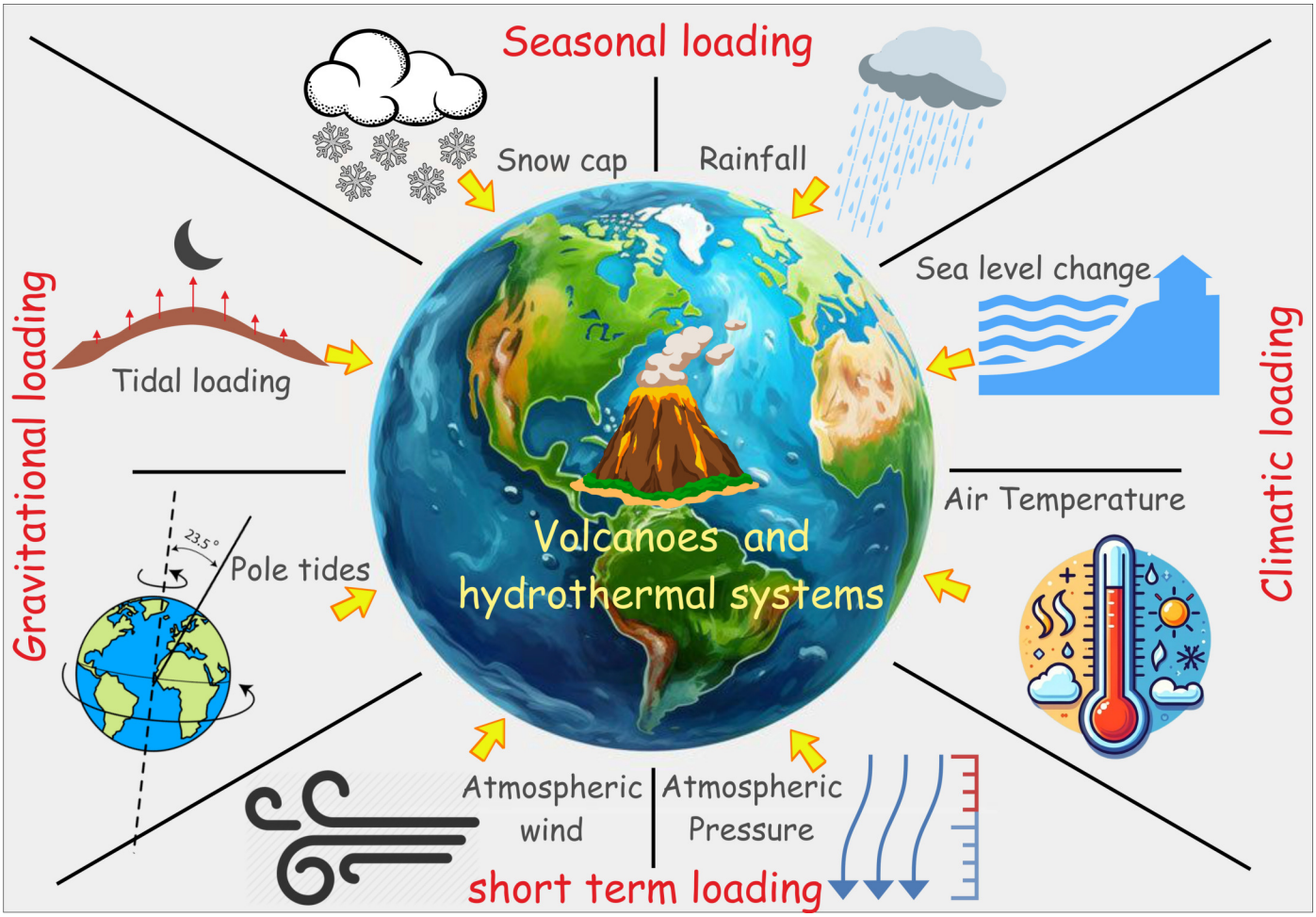

Figure 1. Common natural forces acting on the earth's surface as well as magmatic systems around the globe on semi-diurnal/diurnal (Temperature, pressure, Tides), fortnightly and monthly (Tides); seasonal (Rainfall, snow cap) and multi-annual (Sea level; pole tides; Temperature, pressure) timescales.

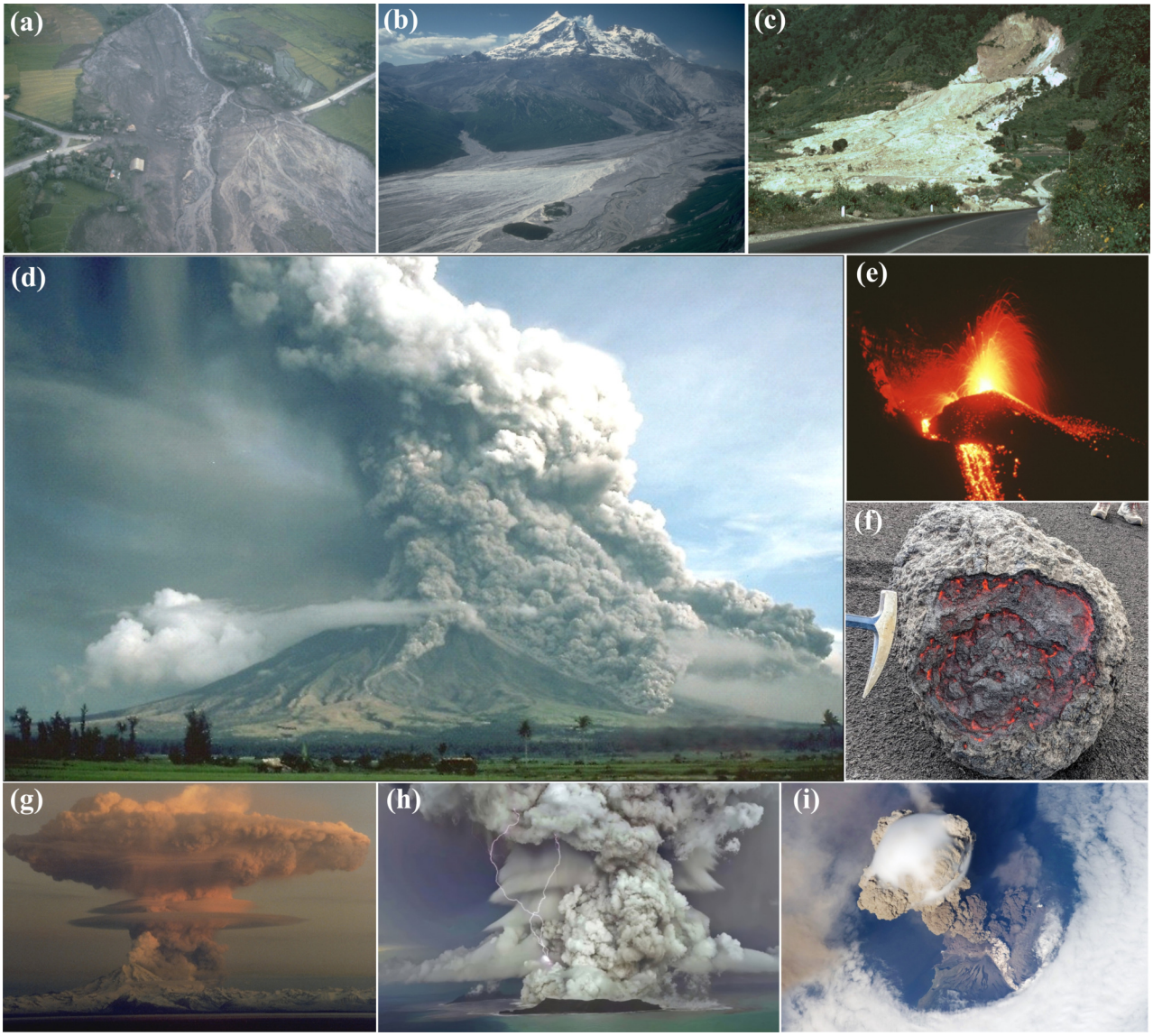

Figure 2. (**a**) Lahars from the 1984 eruption of Mayon volcano (**b**) upper Drift River valley following the 1989–90 eruptions of Redoubt (**c**) The 80-meter-high headwall scarp resulted from the landslide that occurred on 5 January 1991, at Almolonga Volcano within the Zunil Geothermal Field. (**d**) Representation of different hazards from the image of Mt Mayon eruption, Philippines (**e**) Strombolian eruptions at a spatter cone in Pacaya's MacKenney crater (**f**) image of a Volcanic bomb (**g**) The 18 December eruption of Redoubt, viewed from the Kenai Peninsula across Cook Inlet, shows an umbrella cloud that seems to emerge from a vent on the northern flank but is actually ash that rose to more than 10 kms produced by a pyroclastic flow (**h**) Volcanic lightening produced during the Hunga-Tonga Eruption, 2022 (**i**) A NASA Space Shuttle image captured on 12 June shows an eruption plume from Sarychev Peak in the Kuril Islands, reaching altitudes of 16 to 21 km during its eruptions from 11 to 16 June (taken and modified from Global Volcanism Program https://volcano.si.edu/gallery/ImageCollection.cfm, Last accessed on 15 October 2025).

These events highlight the varied dangers of volcanic eruptions and the importance of preparedness and timely evacuation to reduce fatalities. Historically, the total documented loss of life from volcanic eruptions has been modest (i.e., ∼300,000 since 1600 AD) compared to other natural hazards (i.e., around 50 million) [13]. However, the population growth around active volcanoes and hydrothermal systems has increased interest in eruption prediction and volcanic hazard mitigation, which also requires monitoring these magmatic systems and understanding the associated fluid migration and deformation processes, contributing to unrest activity. To mitigate the impact of volcanic events, it must be prioritized for improving eruption forecasts through innovative observations, advanced methods, and refined models of volcanic processes. Observations through geochemical and geophysical techniques enable the study of volcanic processes across scales, from the microscopic (e.g., magma crystal content) to the macroscopic (e.g., lava flow paths).

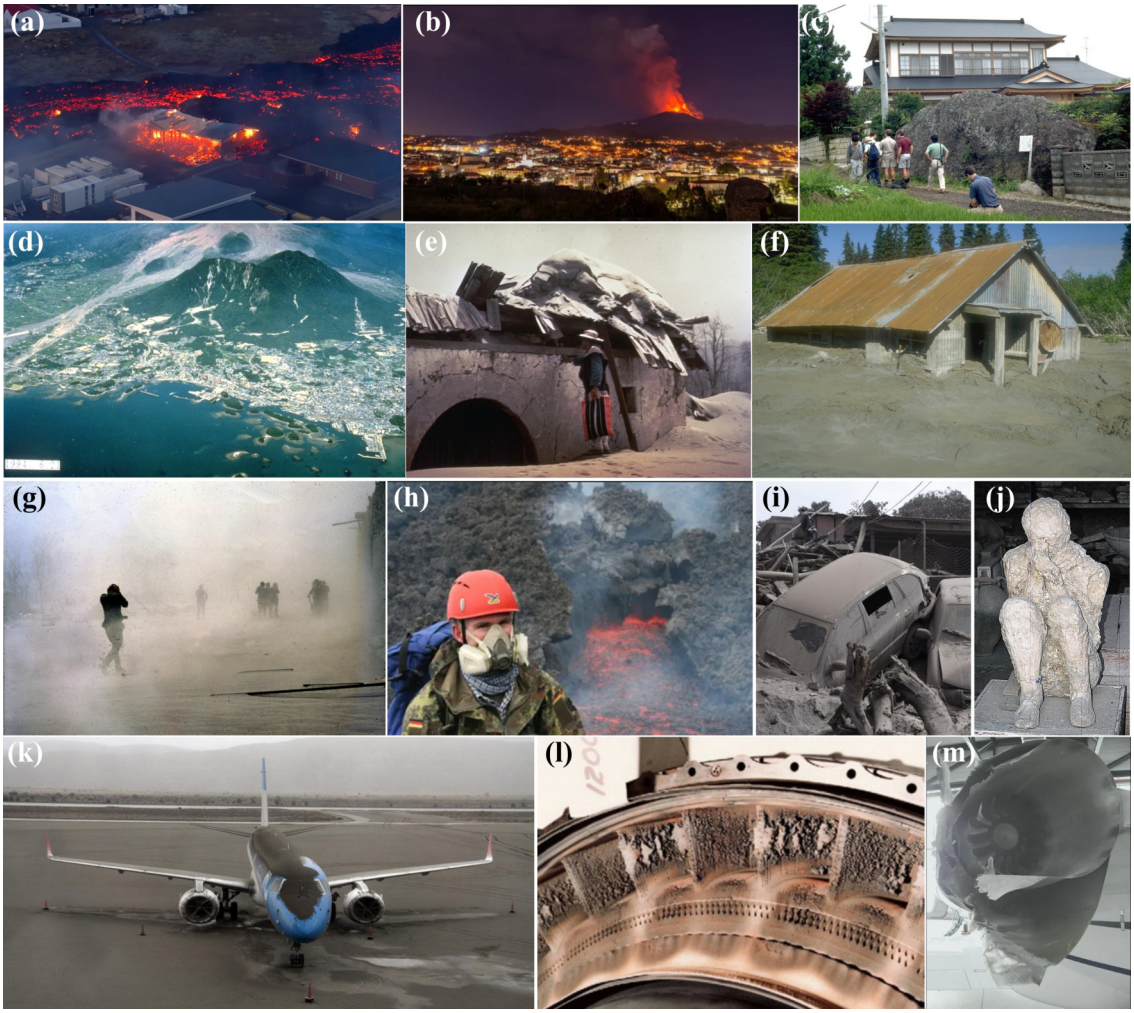

Figure 3. (**a**) Houses getting damaged from the lava flow in Iceland. (**b**) Lava fountains over the eruption at Mount Etna (**c**) Massive boulder carried by pyroclastic flow from Bandai volcano in a lahar during an eruption in 1888 (**d**) The forested islands in Shimabara Harbor were formed by a massive debris avalanche in 1792, originating from Mayuyama, the leftmost of the two forested lava domes behind the city. (**e**) House damaged from the tephra falls in the village of Parícutin (**f**) House damaged by Lahars from the 1989-90 eruptions of Redoubt (**g**) Plumes covering the city from pyroclastic flow at El Naranjo, 7.5 km south of the eruption crater (**h**) Volcanologist using masks to prevent respiratory damages from volcanic gases (**i**) Cars stuck in materials carried by Lahars in Indonesia (**j**) remains of a human body buried in ash at Pompeii. (**k**) Airplane damage due to volcanic ash from Copahue volcano, Chile (**l**,**m**) Aircraft engine damage from volcanic ash and tephra (taken and modified from Global Volcanism Program https://volcano.si.edu/gallery/ImageCollection.cfm, Last accessed on 15 October 2025).

Volcano monitoring through geophysical methods employs both ground- and space-based methods. Ground-based techniques include seismic, geodetic (deformation), gas, thermal, hydrologic, potential field, and tomography observations, often supplemented by drones and lightning detection arrays for inaccessible areas (Figure 4). Space-based monitoring, using satellites, provides long-term, global data on heat flux, gas and ash emissions, and deformation, spanning years or decades (Figure 4). Despite advancements in global satellite surveillance, challenges persist in predicting volcanic eruptions. Notably, a quarter of volcanoes with major explosive eruptions since 1979 had no prior activity in the preceding century. This means that some of the most destructive eruptions in the coming decade may occur at volcanoes without instrumental unrest records [14]. Historical data, such as detailed observations from Krakatoa's 1883 eruption—ranging from tide gauge readings and barograph records to ship logs—offer invaluable insights into both local and global impacts. Beyond scientific observations, historical records documenting personal experiences and crisis management provide critical context for understanding magmatic processes and the human dimensions of volcanic disasters [14]. While satellite monitoring enhances our ability to detect changes at active volcanoes, these historical accounts remain essential, offering complementary perspectives on volcanic risks across time. Together, these approaches of monitoring the deformations and magmatic processes enhance our understanding of volcanic systems and improve hazard mitigation efforts.

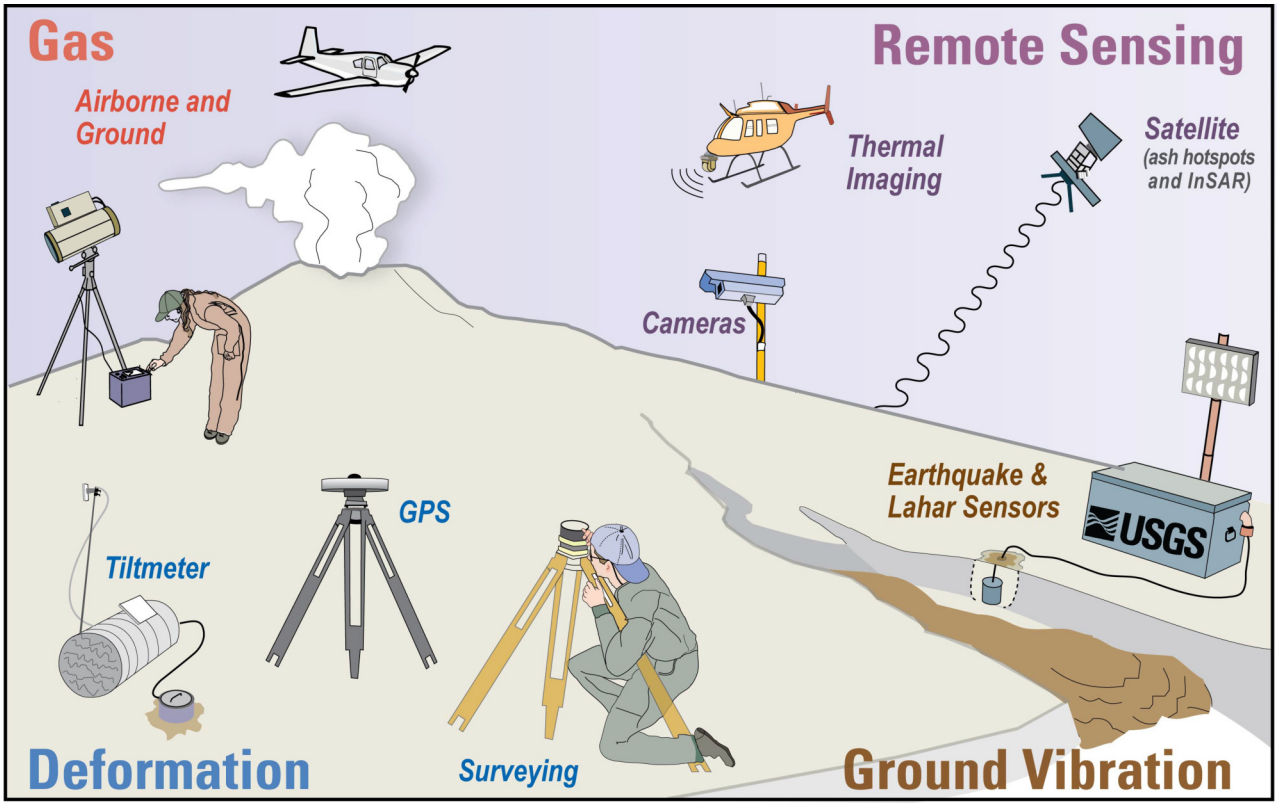

Figure 4. Schematic representation of ground based instruments (GNSS, Tilt meter, Seismometer, Thermal/IR cameras, LiDAR etc.) and air based instruments (InSAR satellites, Airborne imaging and gas measurement through Drones etc.) for volcano deformation monitoring techniques (taken from USGS Volcano hazards program https://www.usgs.gov/vhp, Last accessed on 15 October 2025).

2.2. Volcanic Deformation and Associated Complex Magma Chamber Dynamics

As magma ascends toward the Earth's surface, it deforms the surrounding crust, causing minor or large deformations which can be precisely observed through modern geophysical techniques. Since the shallow crust is brittle, such deformations often trigger earthquakes, which are also readily observed [15]. Magma inflation in the form of crustal deformation and increased seismicity is interpreted as a potential sign of an unrest before the eruption [15]. Therefore, deformation measurements are a crucial tool for studying magmatic processes and monitoring active volcanoes. Alongside seismic monitoring, deformation is a key method for assessing the likelihood of future eruptions with the main goal as to determine the geometry of subsurface magma bodies, such as whether the deformation originates from a dike, sill, equidimensional chamber, or a hybrid source; to quantify key source parameters, including depth, dimensions, volume, and internal magma pressure; and to enhance understanding of the physics behind magma transport and eruption dynamics. Besides, there are several complex processes that govern the internal dynamics of the magmatic system, including the subsurface flow of magmatic fluid, which often has varying melt parameters.

The magmatic systems around the globe differ highly according to the associated tectonic setting, production and composition of magma, fluid pathways, and various lithospheric conditions. Magma transport at depth is controlled by freezing distance, chemical alteration, surficial exposure, and crustal development through repeated injections [1]. Common transport methods include porous flow in partly molten and deformable source rock, fracture flow in elastic-brittle rock, and diapiric ascent of granites through viscous rock, where it is most efficiently transported through cold lithosphere via cracks or dikes. Further, the eruptions can also be influenced by several tectonic triggering processes such as squeezing, bubbling, clamping/unclamping, sloshing, diffusion, and roof failures led by the local tectonics and topographic loading on the caldera system [5]. The process can act alone or in a combined effort to generate an eruption on the surface, which seems too complex to occur but still reaches an average number of around 50 globally each year [16]. Therefore, the crucial monitoring of the surface deformation combined with the seismicity is needed for the clear understanding of the magma chamber and related internal dynamics.

Adding to that, rising magma can be halted for several mechanical reasons. Dikes, for instance, might not reach the surface if the driving pressure is too low, the magma density is too great [17], or if stress zones within the volcanic structure create resistance below the surface. Usually, most systems remain in a state of repose and unrest that could not lead to an eruption generating continuous

surface deformations and seismicity [18]. Further, cooling can cause "thermal death" in dikes by solidifying the magma [18], while decompression can lead to "viscous death" through crystallization that thickens the magma and impedes flow [19]. Sills, where magma flows horizontally, can form when it encounters a stiffness or density barrier or when vertical stress is minimal. Sheeted sills are likely responsible for a large portion of the crust generated along mid-ocean ridges [20]. Dike-sill complexes may combine to produce enormous, partly molten entities that are often linked to the surface via a network of fluid pathways, which includes fractures and faults that are often divided into linked crystal-melt mush zones and melt-dominated areas, known as magma chambers [19]. The distinction between mush and magma is based on whether the material is eruptive. The threshold varies based on crystal size, shape, and strain rate [21]. Rheologically, the system can be classified as partly molten rock below a crucial melt percentage and magma over the threshold [22]. Nevertheless, filling of the magmatic reservoir and increased buoyancy lead to magma ascend, which depends on the evolution of the fluid through several factors such as heat loss, volatile enrichment, assimilation, and properties of surrounding rocks. Understanding of the shallow and the deeper reservoir through precise inverse modelling of the geodetic datasets and seismic studies of the sub-surface system can unveil the prevailing dynamics.

Extensive seismic studies of magmatic systems worldwide have provided detailed images of their structures using inversion methods [23]. These studies reveal that these systems often contain localized magma chambers or accumulated zones above thicker crystal-rich, partially molten rock regions at shallower depths and melt is generated and stored in the deeper crust over long periods before being rapidly transferred to shallow depths when needed [19]. The reservoirs have complex dynamics, involving the permeability, rheology, and fracture pathway structure along with the unconfining or confining nature of the system [24]. Interactions with meteoric or connate water are also evident in the reservoir during fluid transfer, which disrupts fluid mechanics during ascent. Decompression forces from the magma ascent make the dissolved volatile species like water and carbon dioxide expel from the melt, creating bubbles through secondary boiling that may fuel the eruption through degassing. The bubbling is regulated by gas bubble production, magma rheology, and brittle deformation (fragmentation), which can also generate seismicity in the forms of tremors, swarms, and volcano-tectonic events [25]. Also, injection of new magma and overpressure within magma chambers play their roles in the rise of magma to the shallow reservoir and deeper Long period (LP) seismicity [26]. Conclusively, all the processes involving magma properties and their interactions in the conduit are coupled where a consistent correlation exists between fluid buildup at shallower depths (termed inflation) and crustal deformation as vertical uplift. However, it should be mentioned that some volcanoes inflate without exploding, especially at restless silicic calderas, and some eruptions also take place without detectable deformation from the inflation.

Volcano tectonic (VT) events and swarms are the usual seismic events during inflation and eruptive periods, which reach the highest numbers during the pre-eruption [27] (Figure 5). The volcanic unrest phase requires the inflation of the magma chamber due to an increase in overpressure, increase in magma injection, increase in volatile enrichment, or decrease in compressibility of the chamber [2, 28]. The evolution of the volcanic plumbing system for the generation of volcanic activities also impacts the magmatic system's capacity to control the magma storage and interaction with the surrounding rocks [1, 29].

Typically, during the evolution in the degree of inflation of the magma chamber, the rate of deformation and seismicity occurrence increases, which again interacts with the magmatic system (Figures 5 and 6). While the seismic events are substantially micro-seismic and low magnitude $(M < 4)$, higher magnitude events $(M > 5)$ can be accompanied by phreatic eruptions or the release of accumulated sub-surface stress fields due to perturbations from fluid movements during eruption or failures associated with eruption [30, 31]. These increased events are also evident in the form of degassing in the case of volatile-rich magma, where pressure differences between the magma and low-pressure (wall rock) environments can induce fast horizontal gas escape if bubbles within the magma are sufficiently coupled to feed gas to the wall rock [32]. Processes involving chamber inflation during volcanic unrest events and fluid migrations in hydrothermal systems generate crustal deformation (upliftment of the ground surface) and brittle deformation in associated structures (minor ring-fault system and major tectonic fault system) as well as magma-rock interface depending on rock properties [5, 33] (Figures 5 and 6). Also, during eruption the chamber deflation also produces unrest events through negative surface deformation and brittle deformations in the subsequent ring-faults produced due to the collapsing of the chamber roof (Figure 5) [34]. The collapsing or downsag produces outward dipping ring faults which with further peripheral downsags produce inward dipping ring faults. Depending on the stage of inflation/deflation the nature of the ring faults (Normal/reverse) changes according to the deformation pattern [33, 34].

2.3. Eruption Cycles and Caldera Dynamics

Cyclic eruptive cycles in volcanic systems have been detected on both short and long timescales through seismic activity, degassing, and measurements of eruptive frequency and intensity. However, cycles on a longer timescale are detected from changes in the rate of occurrence of volcanic eruptions or changes in eruptive flux [35, 36]. This time scale has been explained by the destruction of an impermeable magma plug when overpressure exceeds a threshold and recrystallization of the plug from combined rheological changes.

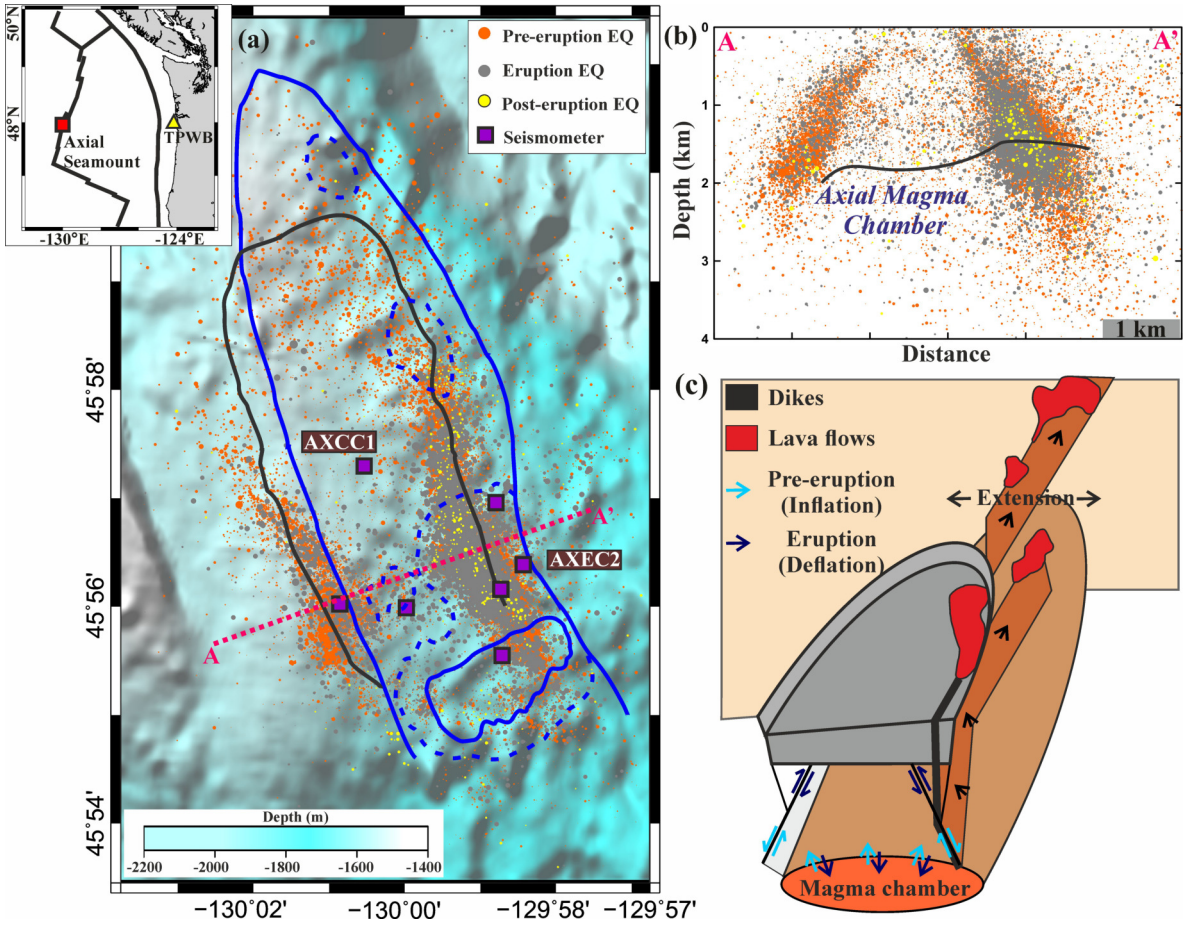

Figure 5. (**a**) Bathymetry and spatial distribution of micro-seismicity, seismic network and collocated bottom pressure recorders (AXCC1 and AXEC2 marked by squares) surrounding the Axial Seamount on the Juan de Fuca ridge. The bathymetry data is archived from General Bathymetric Chart of the oceans (https://www.gmrt.org, Last accessed on 15 October 2025). Seismicity distributions during three phases of eruptions (i.e., pre-eruption, eruption and post-eruption) are marked by different colors and symbol sizes are scaled by magnitude of earthquakes. The caldera rim (black line), surface trace of the magma chamber (blue solid line) and depth contours for at depth of 1.5 km (dashed blue line) below the seafloor are highlighted. Inset shows locations of the Axial Seamount (red square) and tide gauge station (yellow triangle) at the coast of Cascadia Subduction zone (archived at https://www.ncei.noaa.gov/maps/hazards/?layers=0, Last accessed on 15 October 2025). (**b**) Vertical cross section (AA' in Figure 5**a**) across the caldera region showing depth profile of earthquake distribution. Roof of the Axial Magma Chamber is marked by solid black line. (**c**) Schematic representation of dynamics of the caldera, dikes and nature of faulting. During pre-eruption stage magma chamber, inflation dominates producing normal fault earthquakes and reverse fault motion occurs during the eruption stage where magma chamber deflation dominates (Modified after [27]).

The overall timescales can be divided into Pre (inflation), Syn (deflation), and Post (Repose) eruption periods according to the magmatic system's magma inflation/deflation stage (Figure 6). Small periods ranging in days are often hard to discriminate due to the sudden release of fluids without any unrest signature. Intermediate periods are characterized by multiple-week cycles of earthquakes, tilt, and eruptive activity, which can be explained by dikes opening and reopening due to pressure variations. Over a longer timescale, dome development and quiescence alternate with multiple years. Long-term scale behavior may be described in the magma chamber and conduit operate as energy reservoirs due to the elastic deformation of the wall rocks, releasing magma episodically when pressure exceeds a certain threshold. The time scale for this process follows the elastic relaxation of the chamber, with longer times resulting from bigger chamber sizes. When the threshold is exceeded, the magmatic system goes into volcanic instability, in which a volcanic structure has been sufficiently destabilized to raise the possibility of the structure failing whole or in part. Also, using finite element modeling, it has been proposed in case of a cycle of instability: after the instability or eruption, the removal of material causes the impermeable wall rock of the magma chamber to behave elastically in the initial period and later on in the repose period, the relaxation of the chamber wall creates the pressure difference for the magma flow from the deep source into the chamber [15].

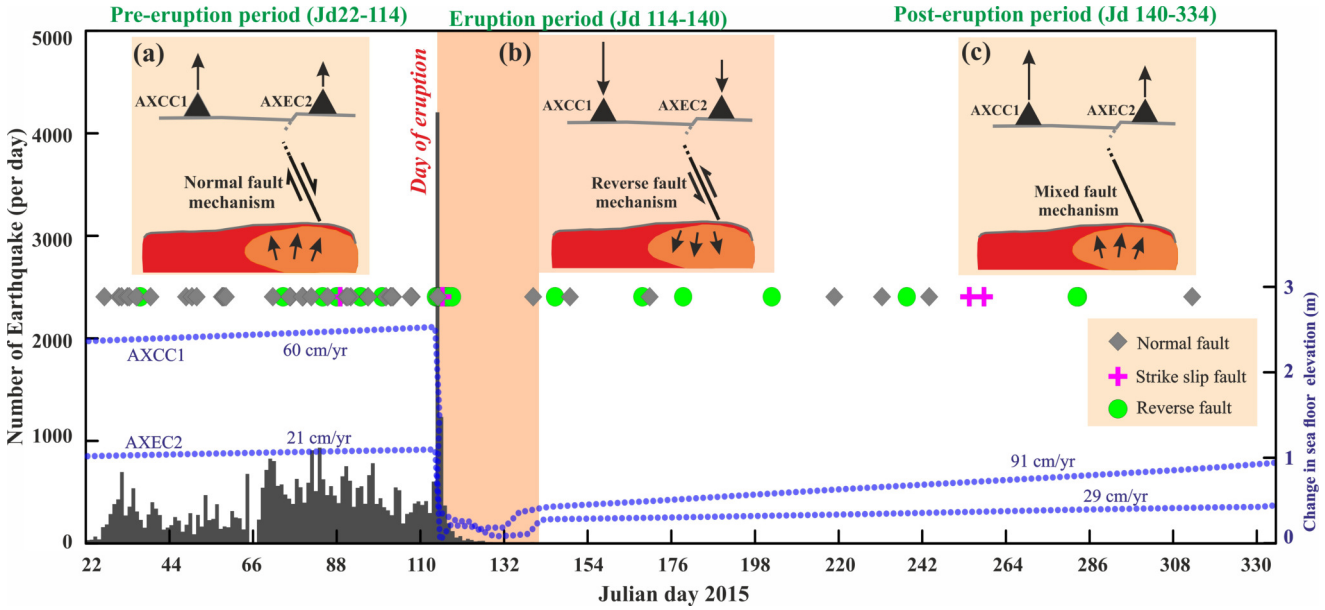

Figure 6. Temporal representation of three phases of eruption sequences (i.e., pre-eruption, eruption and post-eruption) at the Axial Seamount on the Juan de Fuca ridge. The change in sea floor elevation (dashed blue lines) was obtained from two bottom pressure recorder stations AXCC1 and AXEC2 (marked in Figure 5**a**) and daily earthquake distribution during Pre-eruption (Jd: 22–114, 22 January–24 April), Eruption (Jd: 114–140, 24 April–20 May) and Post-eruption (Jd: 140–334, 20 May–30 Nov) phases. Focal mechanism solution types are marked by different symbols (Normal: Grey diamonds; Reverse: Green circles; Strike slip: Pink crosses). Note that during pre-eruption and eruption phases, normal and reverse type of earthquakes dominate, however during post-eruption phase mixed types of earthquakes are recorded (Modified after [27]).

Failures in the surrounding host and cap rocks of the magma chamber generate caldera or ring faults through subsidence which are critical in generating an eruption, acting as the fluid transfer conduit [5, 34]. The subsidence again compresses the magma chamber, and the fractures can undergo healing processes, which confine the chamber and allow it to re-inflate due to endogenous processes in a cyclic manner [23]. During the process the caldera ring faults may produce complex seismogenic fault mechanisms which differ according to the phase/stage of the eruption cycle (Figure 6). Usually, the normal fault mechanisms dominate during the pre-eruptive inflation stage and reverse faulting during the eruptive roof collapse stage (Figures 5 and 6). However complex combinations can be observed with presence or absence of shallow hydrothermal systems and evolution of the caldera ring fault during the different stages in an open or closed system [27, 34] (Figures 5 and 6).

2.4. Triggering and Modulation of Volcanic Activity

Several studies have shown that volcanoes are complex systems on which the dynamics are often determined by the interplay between magmatic and the externally acting natural forces [7, 8, 10, 31, 37]. Further, eruptions can also be influenced by several tectonic and magmatic triggering mechanisms, which may act independently or interactively to initiate surface activity. To provide conceptual clarity, the processes influencing volcanic unrest can be broadly understood in terms of background signals, modulation, and triggering mechanisms. The background signals represent the long-term or quasi-steady endogenous processes within a magmatic system, such as magma accumulation, degassing, and gradual crustal deformation, which define the baseline state of stress and energy buildup. Modulation processes, in contrast, refer to external or cyclical factors that modify or amplify these background trends without directly initiating eruptive activity. These can be broadly categorized as follows:

(a) Endogenous (internal) mechanisms:

- Overpressure and magma injection: Excess pressure from magma replenishment or volatile accumulation within the reservoir.
- Bubbling and degassing: Gas nucleation and bubble expansion that modify magma rheology and chamber pressure.
- Sloshing or magma oscillation: Resonant oscillations within conduits or reservoirs that enhance instability.
- Diffusion and volatile enrichment: Changes in melt composition and volatile content influencing magma buoyancy and transport.

(b) Exogenous (external or structural) mechanisms:

- Clamping and unclamping by regional stress fields: Stress changes from tectonic loading or unloading that affect dike propagation.

- Roof collapse and chamber-cap failure: Brittle failure of the chamber roof due to overpressure, subsidence, or gravitational instability.
- Topographic or caldera loading effects: Stress contributions from edifice weight, sediment accumulation, or hydrothermal sealing.

These interacting processes collectively govern the onset and evolution of volcanic unrest. The combination of internal magmatic overpressure with external stress modulation can therefore explain the temporal clustering of deformation and seismicity preceding eruptions [1, 5].

The external stress perturbing agents include various processes such as rainfall-induced seasonal changes of pore fluid pore pressure [11, 31, 37, 38], seasonal loading/unloading due to the fluctuations in water table and ice cap [39, 40], seasonal atmospheric pressure and thermal cycles contributing to the variation of the lithostatic pressure and ground temperature [8, 41], earth rotation as well as pole tides [12, 42], wind speeds affecting the surface load [9] and tidal loading [27, 30, 31] as well as sea level changes [10].

The modulating agents can be divided into short-term (Lunisolar tidal, seasonal) and long-term (Climatic, pole tidal) agents which act on the different time-scales on the active volcanoes. Magmatic systems with eruptive activity over a longer time scale with dome development and quiescence alternating with multiple years can have the long-term climatic or astronomical influence through the stress perturbations. Seasonal rainfall modulations are reported from various active volcanoes and even non-volcanic tremors [38, 39]. Similarly, tidally triggered non-volcanic tremors are reported worldwide [43]. Theoretically, short-period stress perturbations as tidal modulations can occur in a system with high loading velocity and constant periodic tidal loading, which can only be achieved during a critical state of inflation of the magma chamber [44, 45]. Also, as interpreted from the resonance destabilization concept, the anomalous fluid-rich crust could put the fault segments or deformation zones in the conditionally stable frictional regime. Fluid transfers in this regime, as well as crustal deformations and eruption events, including seismicity, are susceptible to recurring exogenous forces, primarily driven by seasonal hydrological and tidal loading [45].

As a specific response, the possibility of periodic or quasi-periodic behaviors at certain volcanoes [8, 10] in response to lunisolar tidal forces [46], including the diurnal, semi-diurnal, or fortnight tides, results in an increase in the likelihood of eruption onset or associated deformations, explicitly when the volcanoes are in a critical state [10]. The susceptibility of a volcano to external forcing largely depends on whether it is in a critical state—a condition where the internal pressure and stress within the magmatic or hydrothermal system approach the mechanical failure threshold of the surrounding crust. This criticality is governed by several interrelated parameters, including magma chamber overpressure, volatile content and gas saturation, magma viscosity, crustal permeability, and ambient tectonic stress. As inflation progresses, overpressure reduces the effective normal stress along existing fractures and faults, making them more prone to slip or dilation. Likewise, volatile enrichment enhances buoyancy and chamber pressurization, while transient permeability increases enable fluid migration that further destabilizes the volcanic edifice. A volcano in such a state becomes highly sensitive to even small external stress perturbations, typically ranging between 1–10 kPa, caused by tidal loading, rainfall, or atmospheric pressure variations. These perturbations can transiently modify the local stress field, resulting in enhanced seismicity, degassing bursts, or even eruption onset. Identifying a system nearing this critical state requires integrated multi-parametric monitoring using seismic, geodetic, and geochemical observations. Characteristic indicators include accelerated ground inflation, increasing micro-seismic activity, shifts in gas emission ratios, and evolving frequency-dependent deformation patterns. Notably, nonlinear deformation acceleration, sudden changes in uplift or tilt rate, and rising long-period (LP) seismicity often mark the transition toward critical behavior.

Once a volcano reaches this critical stress equilibrium, external forces can modulate its response in a quasi-periodic or transient manner, producing observable correlations between environmental cycles and internal unrest signatures such as seismic swarms or deformation bursts. The combined contributions from exogenous forces cannot be accurately estimated; however, the individual contributions from the primary sources of rainfall, Snow loading, and tidal loading can be accurately estimated through various modelling and estimation techniques. It has long been recognized that large volcanic eruptions can influence climate, a phenomenon known as “volcano-climate impacts,” which remains a significant area of research [47]. The reverse question, how climate change impacts volcanic processes—referred to as “climate-volcano impacts”—is also not new. The modulation of volcanic activity on seasonal timescales in the modern era suggests that current processes may provide a real-time analogue for phenomena once believed to occur only over geological time. This includes events such as the onset of glaciations and the associated rapid sea-level drops [48], deglaciation and ice removal in Iceland [49] and eastern California [50], as well as changes in sea level rates in the Mediterranean [51]. Decades ago, it was hypothesized that deglaciation or changes in sea level could influence volcanic activity. Variations in the distribution of surface load can result from factors such as ice cap melting, sediment deposition and erosion, changes in precipitation intensity, surface water storage, and sea-level fluctuations. These variations alter the stress state in the Earth’s crust and potentially extend into the upper mantle, affecting pressure, deviatoric stresses, and stress orientation. Such changes can, in turn, influence magma production, transport, and eruption e.g., [39, 40, 52].

The seasonal timescales can be observed both on snow loading as well as meteoric water loading from rainfall which are evident on the global eruption catalogues, especially on the VEI > 1 events [39] (Figures 7 and 8). Snow loading and subsequent seasonal changes have been linked to volcanic activity in several regions. At Mount St. Helens in the USA, winter snow accumulation increases surface stress on the volcanic edifice, while spring snowmelt reduces this load, potentially influencing magma movement and seismicity [53]. Similarly, at Mount Ruapehu in New Zealand, snow and ice dynamics affect hydrothermal systems, with seasonal snowmelt promoting phreatic explosions or impacting eruption timing [54]. In Klyuchevskoy Volcano in Russia, spring snowmelt infiltrates the volcanic system, raising pore pressure and increasing the likelihood of seismic activity or eruptions [55]. For Katla Volcano in Iceland, seasonal snow and glacier meltwater can penetrate the crust, modulating hydrothermal systems and triggering seismic unrest [56]. At Yellowstone Caldera in the USA, snowmelt contributes to seasonal hydrothermal changes by altering subsurface fluid pressures, which can influence seismic and geothermal activity [57].

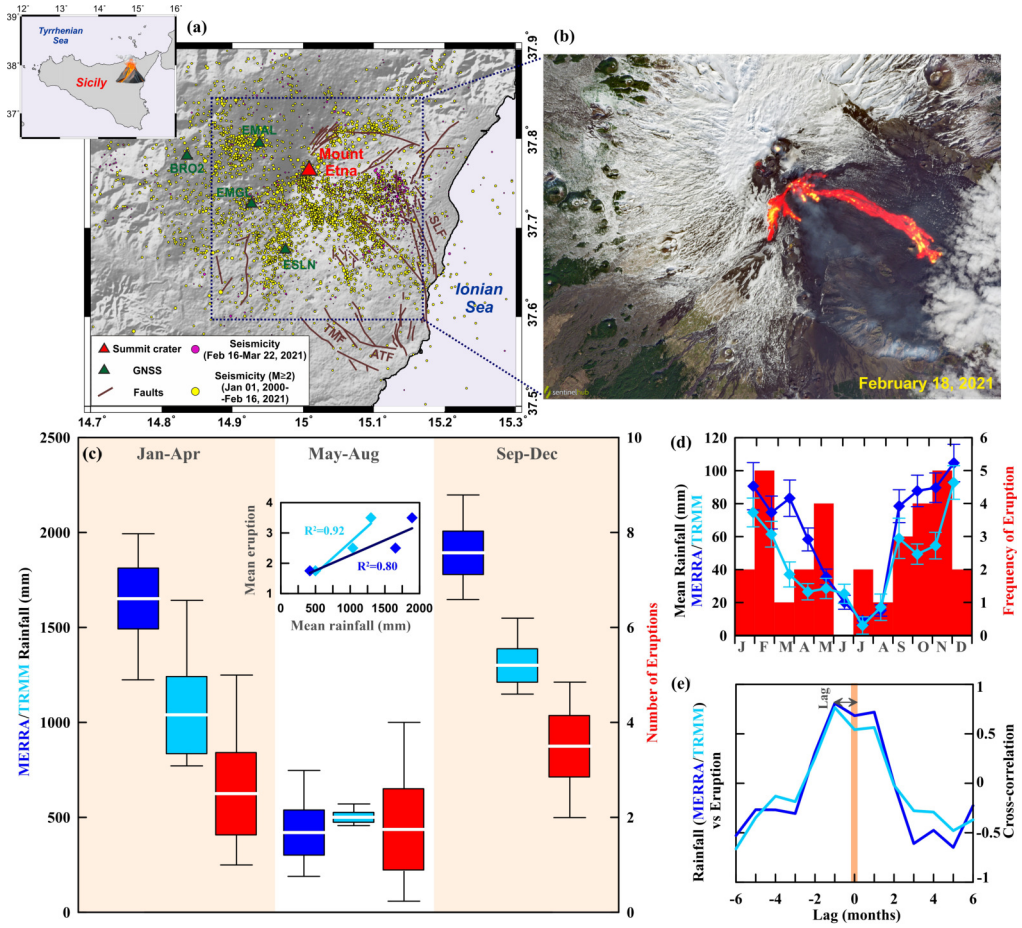

Figure 7. (**a**) Topographical map of Mount Etna (Italy) with the tectonic features and faults. Red triangle shows the summit crater of Mount Etna. Seismicity events surrounding the crater are represented by two different coloured circles, separating events prior to and after the recent 16 February 2021 eruption sequence. Green triangles represent a small section of the available GNSS stations. Inset shows the location of Mount Etna from Sicily, Italy. SLF: San Leonardello Fault; ATF: Acitrezza Fault; TMF: Tremestieri Fault. (**b**) Enlarged satellite view of the Mount Etna volcano showing eruption activity obtained from Copernicus Sentinel-2 data acquired on 18 February 2021 (marked by dashed rectangle in Figure 7**a**). (**c**) Four-month distribution of rainfall (both MERRA, 2000–2021 and TRMM, 2000–2020) and eruption events at Mount Etna (1600–2021) are represented by Box and Whisker plot. The white line within the box denotes the arithmetic mean value, and the upper/lower extremes of the box indicate the values of the standard error of the mean, and the black lines of the box denote the minimum/maximum values of the corresponding rainfall and eruption events. Note that the higher number of eruptions occurs mainly during the wet season. Inset shows the linear correlation between the mean eruption and mean rainfall values, which shows a good statistical correlation with a high R^2value. (**d**) Monthly distribution of mean rainfall from both MERRA and TRMM sources and eruption events. (**e**) Cross-correlation between rainfall (MERRA: blue line and TRMM: cyan line) and eruption events, with strong cross-correlation with a lag of $\sim$1–1.5 months (Modified after [37]).

The relationship between sea-level changes and volcanic activity has been widely studied, offering diverse insights into this interaction. Rampino et al. [48] first hypothesized that rapid sea-level drops during glaciations could trigger volcanic eruptions by reducing lithostatic pressure and inducing decompression melting in magma chambers. Jull and McKenzie [49] supported this with evidence from Iceland, showing how ice cap removal during deglaciation caused crustal rebound and increased eruptions around 10,000 years ago. Glazner et al. [50] linked ice sheet melting to volcanic activity in eastern California, emphasizing regional variations in response to stress reduction. Similarly, McGuire et al. [51] correlated Holocene sea-level changes in the Mediterranean with increased volcanic activity due to stress redistribution from sediment erosion and deposition. Mason et al. [39] found a global correlation between volcanic seasonality and sea-level changes, while Sigmundsson et al. [40] quantified crustal stress changes from historical sea-level variations, showing that rising sea levels could suppress activity. Watt et al. [52] examined sea-level-induced stress redistribution on magma transport, and Satow et al. [58] used numerical models to show that tensile stress from sea-level falls drives dyke eruptions at Santorini (Figure 9).

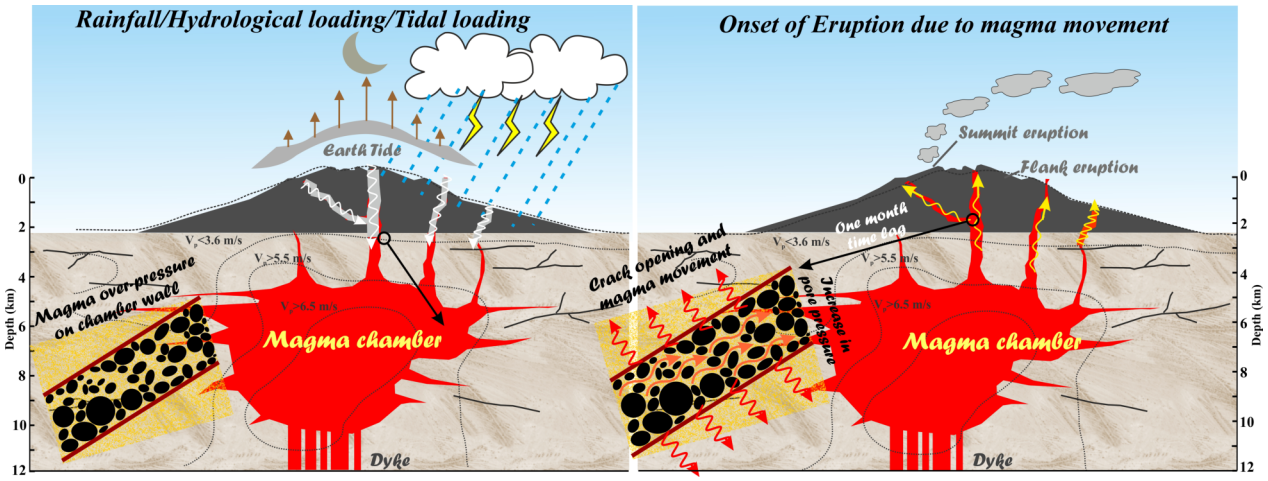

Figure 8. The schematic diagram represents the role of tidal loading, regional rainfall, and associated hydrological loading with the onset of eruption at Mount Etna (Italy). During the wet season, heavy rainfall and associated hydrological load significantly weakens the volcano edifice, initiates mechanical tensile failure, and causes an increase in pore pressure along the fissure channels and adjacent walls of the complex magmatic system. This promotes dyke intrusion and eventually triggers the eruption cycle. The tomographic contours (black dashed lines) are p-wave velocity (V_p). (Modified after [37].)

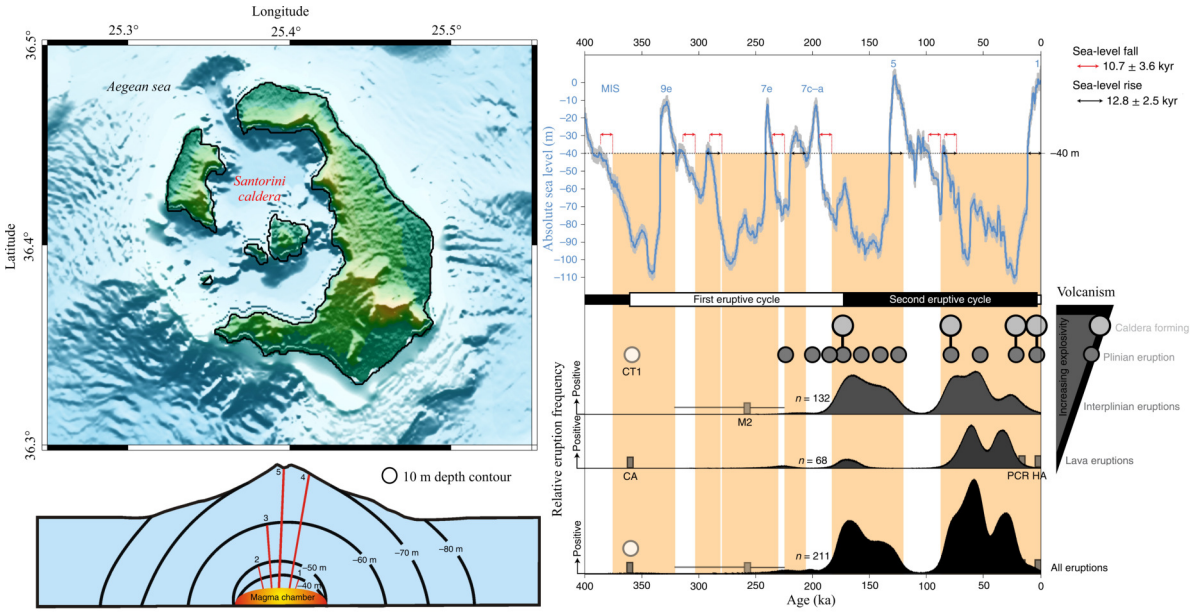

Figure 9. (**a**) Location and topography of the Santorini caldera, Greece. (**b**) Conceptual figure of decrease in hydrostatic load during sea level fall along with the decay effects considered through Green's functions using which accurate stress drop values are calculated with sea level change in the Aegean Sea.

In the past few decades, coupled hydro-mechanical and poro-mechanical process has been linked with diverse geological phenomenon including, weakening of seismogenic faults, aftershocks occurrence [59], seismic swarm [60], slow-slip events [61], hydro-thermal seismicity [62], induced seismicity (including both natural or Human-induced earthquake) [38, 63], seasonal deformation [64], landslides [65] etc. in various geological settings. In fact, compselling evidence exists for rainfall-triggered volcanic-seismicity [66], hydro-magmatic system with infiltrating rainwater causing gravitational dome collapse [67], extreme rainfall-triggered rift eruption [11], rainfall-induced hydrological loading and unloading on the volcanic edifice [31, 37, 68], and generation of lahars and associated flow mechanism [67].

Recent observations increasingly highlight the role of rainfall-induced stress variations in modulating ground deformation and seismic activity. Meteoric water storage and load can deform the surface, induce crustal stresses, and influence seismicity. Rainfall-induced pore-fluid pressure variations also promote ground deformation [69] and can trigger earthquake nucleation, often exhibiting seasonal patterns correlated with precipitation [38]. In volcanic environments, rainfall modulation assumes particular importance as it interacts with the internal magmatic processes, potentially affecting volcano dynamics. For volcanoes experiencing magmatic or hydrothermal unrest, meteoric water can act as a trigger for volcanic activity on timescales ranging from hours to months. For example, at Nevado del Ruiz (Colombia), interactions between meteoric water loads and groundwater likely caused deformation events and triggered phreatic explosions and seismicity between 1985 and 1988 [70]. A study of over 150 years of eruptions at Piton de la Fournaise (La Réunion) suggested a possible link with rainfall, supported by models of ground deformation due to water loading/unloading [68]. At Soufrière Hills volcano (Montserrat, Lesser Antilles), seismic activity during 2001–2003 was influenced by intense rainfall, attributed to water percolation into cracks and interactions at shallow and deep levels over hours to days [66] (Figures 7 and 8). The study concluded that rainfall modulates pre-existing internal processes rather than initiating new events. Extreme rainfall is also believed to have triggered the 2018 rift eruption at Kīlauea volcano (Hawaii) by increasing pore pressure at depths of 1–3 km, leading to mechanical failure of the volcanic edifice [11] (Figures 7 and 8). Notably, this eruption was not caused by magma intrusion but by dyke propagation induced by meteoric water infiltration. Historical data further supports a statistical correlation between rainfall and volcanic activity at Kīlauea and Mount Etna [11, 37] (Figures 7 and 8). As the meteoric water from the rainfall percolates to the ground surface to add up the lithospheric loading as well as generate mechanical failures on the caldera structure, the mechanisms related to the rainfall modulated activity are reported to be complex in nature (Figure 8).

This synthesis underscores that external forcing operates hierarchically across multiple timescales (Table 1). Short-term loads such as tides and atmospheric variations modulate unrest in critically stressed systems, while seasonal and climatic factors rainfall, snowmelt, and sea-level fluctuations alter crustal stresses and pore-fluid pressures on intermediate timescales. Over geological timescales, glacial cycles and tidal forcing reshape the lithospheric stress regime, influencing magma production and eruption frequency. Recognizing these coupled internal–external feedbacks is crucial for improving predictive models of volcanic and hydrothermal hazards under changing climatic conditions.

2.5. Hydrothermal Systems and Effect of Tidal Loading on Fluid Flow

Hydrothermal systems, occurring in diverse tectonic settings, are intrinsically linked to varying seismic characteristics. These systems, marked by interactions between heat, fluids, and rock, often generate seismicity influenced by local tectonic conditions, fluid migration, and thermal processes. Fluid-dominated seismic swarms are a hallmark of hydrothermal systems, reflecting the critical role of fluid pressure changes within faults and fractures. These swarms are typically characterized by clusters of small- to moderate-magnitude earthquakes occurring over days to months, primarily driven by the migration of pressurized fluids and their interactions with the surrounding rock matrix. In extensional tectonic settings, such as rift zones and mid-ocean ridges, fluid-driven swarms are common. For example, in the East African Rift System, swarms have been attributed to the intrusion of magmatic fluids into crustal fractures, creating overpressures that reduce fault strength and trigger seismicity [71]. Similarly, along the mid-ocean ridges, hydrothermal vent systems often exhibit swarms as circulating fluids interact with the newly formed crust. In subduction zones, where fluids are released from dehydrating slabs, seismic swarms often mark the migration of these fluids through the overriding plate. At the Cascadia and Nankai subduction zones, studies have shown that transient fluid pressure pulses within faults can generate swarms of low-frequency earthquakes and tremors [61]. These events highlight the role of fluid overpressure in fault slip dynamics. Transform fault systems also show swarms linked to episodic fluid flow. For instance, along the San Andreas Fault, fluid pulses within fault zones can drive localized swarms, as fluids temporarily reduce the effective normal stress, promoting shear slip. These events are often short-lived but provide valuable insights into fault-valve behavior.

Volcanic hydrothermal systems are particularly prone to fluid-dominated swarms due to intense interactions between magmatic and hydrothermal fluids. At Yellowstone, frequent swarms have been linked to the pressurization and movement of hydrothermal fluids within the shallow crust [72]. Similarly, swarms at Mount Ontake, Japan, are driven by the upward migration of supercritical fluids, often preceding or accompanying phreatic eruptions [73]. These serve as dynamic indicators of fluid migration and overpressure within hydrothermal systems where they vary

across tectonic environments but consistently emphasize the critical role of fluid-induced stress perturbations in driving seismicity.

Several natural forces are acting in and on Earth that provide stress perturbations on deformation plane to generate failure. However, the gravitational attraction from the moon and sun during rotational cycles in particular orbits create deformations leading to periodic fluctuations on Earth surface. At ocean surface these are defined as Ocean tides and on the rigid earth surface as body tides. Deciphering the law of gravitational attraction, mass of the Moon is much smaller (roughly 27 million times) than that of the Sun, but the distance of earth to the Sun is much greater (roughly 400 times) making the lunar tidal effect much greater than the Solar [74]. Tidal loadings are a prominent source of periodic stress variation on the Earth's surface. Predominantly, there are 37 major tidal constituents with 32 short-period (J1, K1, K2, L2, LAM2, M1, M2, M3, M4, M8, MK3, 2MK3, MN4, MS4, MU2, N2, 2N2, NU2, O1, OO1, P1, Q1, 2Q1, R2, RHO, S1, S2, S4, S6, 2SM2, T2) and five long-period constituents (SSA, SA, MM, MF, and MSF) [75]. These lunisolar gravitational forces produce periodic tidal loading at various stress intensities and periods. Earth tidal loading can be lower as compared to ocean tidal load, but with the presence of the majority of hydrothermal systems under submarine conditions, the influence of tidal loadings is exceptional [4, 30, 76]. The loadings provided by tides cannot be large enough to initiate seismogenic events, but the constant, periodic nature of the load can trigger or modulate seismogenic activities such as deformations through fluid movement in fractures or cracks [46] (Figure 10). Temporal variations in fluid migration can be expected due to tidal loadings at the hydrothermal system due to the susceptibility of fluids to even low-magnitude stress that is constant and periodic [76]. The movement response due to tidal loadings is controlled by the medium's poroelasticity and the composition of the interstitial fluids, which can act as fluid pathways. Further, mixing hydrothermal fluids supports the low-temperature diffused discharge through leaking or secondary circulation, which is crucial for the influence of tidal loadings.

Table 1. Summary of exogenous stress-modulating mechanisms that influence magmatic and hydrothermal systems across multiple temporal scales.

Timescale	Triggering/Modulating Factor	Primary Mechanism	Representative Regions/Examples	Key References
Hours–Days (Short-term)	Lunisolar tidal loading	Periodic stress perturbations (10^{-3}–10^{-2} MPa) influencing dike and fault stability	Mount St. Helens, Campi Flegrei, East Pacific Rise	McNutt & Beavan [30]; Wilcock et al. [7]; Sahoo et al. [76]
	Atmospheric pressure fluctuations	Surface stress modulation affecting shallow hydrothermal systems	Nisyros Caldera, Yellowstone	Petrosino et al. [8]
Days–Months (Seasonal)	Rainfall and pore-pressure variations	Infiltration alters lithostatic load or unclamps fractures, triggering fluid flow or failure	Kīlauea, Mount Etna, Soufrière Hills	Farquharson & Amelung [11]; Matthews et al. [66]
	Snow and ice loading / melt	Cyclic loading–unloading changes crustal stress and magma ascent pathways	Katla, Mount St. Helens, Ruapehu	Sigmundsson et al. [40]; Hurst & Smith [54]
Years–Millennia (Long-term)	Sea-level variations	Hydrostatic pressure change influencing magma chamber stability and melt generation	Santorini, Icelandic volcanic systems	Watt et al. [52]; Jull & McKenzie [49]
	Deglaciation and glacial rebound	Crustal unloading and decompression melting	Iceland, Alaska	McGuire et al. [51]; Mason et al. [39]
	Orbital (Milankovitch) cycles	Long-term modulation of crustal stress and volcanic frequency	Global volcanic belts	Sottili et al. [12]

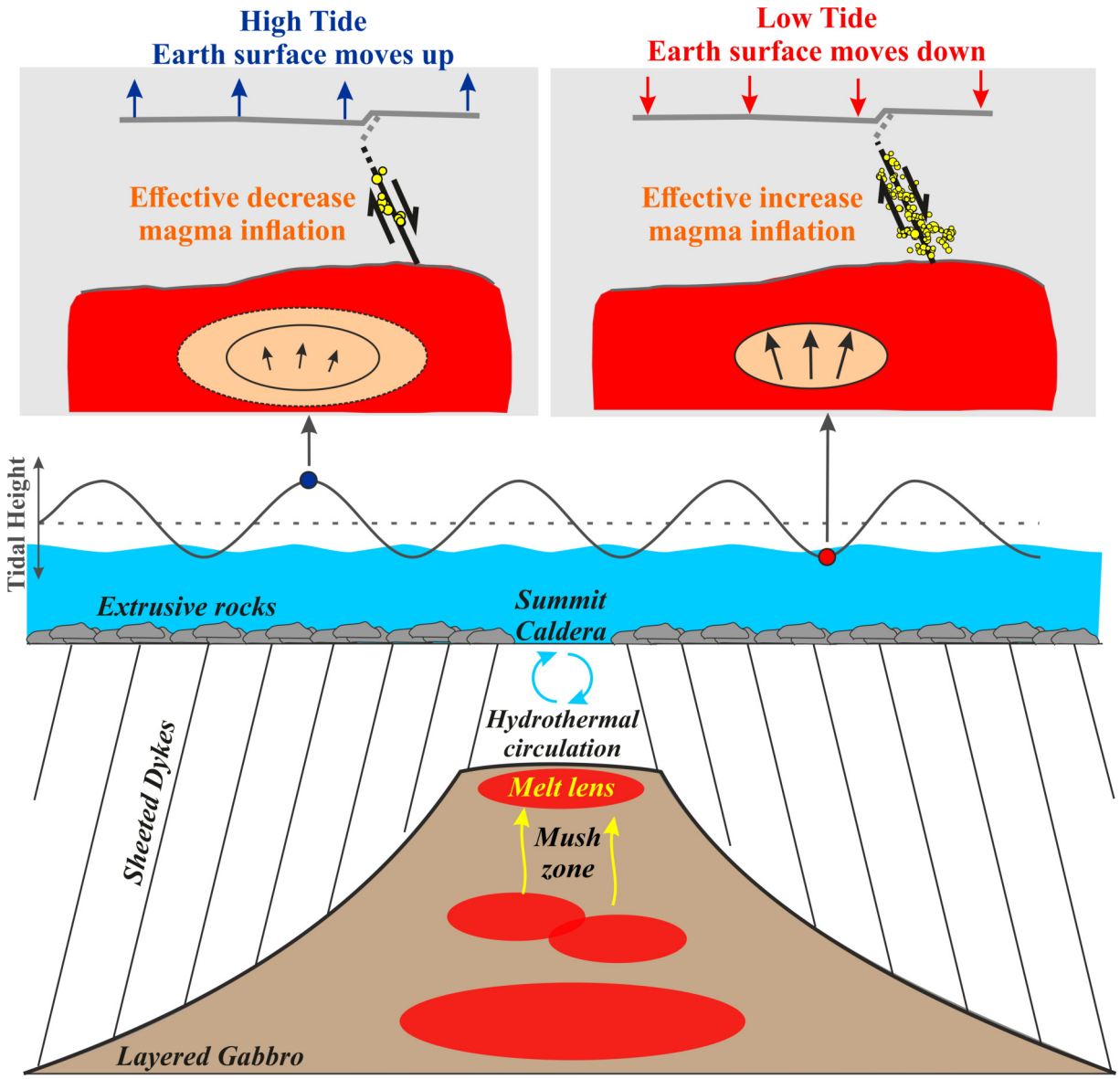

Figure 10. Schematic conceptual model illustrating the dynamics of submarine magma chamber and the influence of tidal forcing on it at the Axial seamount submarine volcano in Juan de Fuca ridge, NE Pacific. In case of high tide, there is an effective decrease in magma chamber inflation, whereas for low tide there is significant increase in magma chamber inflation. The effective increase in magma chamber inflation during low tide, promotes normal faulting earthquakes due to increase in the ΔCFS (Coulomb Failure Stress) (Modified after [27]).

For instance, at Campi Flegrei Caldera (Italy), observations show that semi-diurnal (M2) and diurnal (K1) tidal components periodically alter pore pressure within the shallow hydrothermal system. During high-tide phases, compressional stresses inhibit upward fluid flow, while low-tide unloading enhances permeability and triggers microseismic swarms linked to gas and vapor movement [8, 31]. Similarly, along the East Pacific Rise, fortnightly (Mf) tidal cycles modulate hydrothermal venting rates and microseismicity, where low-tide periods correspond to dilatational stress conditions that promote enhanced circulation of hydrothermal fluids through crustal fractures [7, 77]. These examples demonstrate that the amplitude and frequency of specific tidal constituents can directly govern the timing and intensity of fluid migration in both continental and submarine hydrothermal environments. Even though the absolute stress magnitudes are small (typically $\sim$0.001–0.01 MPa), their continuous and periodic nature enables them to act as effective modulators of permeability and pressure within critically stressed magmatic–hydrothermal systems.

The water level data from the tide gauges can also be used to estimate the ocean tide loading at ocean bottoms using similar principles. This leads to a possible correlation analysis of the hydrothermal activity and deformation through fluid circulation. Hydrothermal earthquakes, which occur due to hydrofracturing by fluids, mainly occur in swarms in the lower crust. These are small-magnitude

events that are substantially modulated by tidal loadings [4, 27, 76] (Figure 10). Again, the role of depth in tidal stress effects highlights key variations in stress distribution and its significance for seismicity. Radial and shear stress components increase monotonously with depth, reaching their highest values in the mid-mantle (1000–2000 km), although this range lies far below the maximum earthquake focus depth of ∼684 km [78]. Up to 1000 km depth, the distribution of tidal stress components shows minimal dependence on Earth's internal structure, with differences between the PREM and homogeneous mantle models remaining below 20% [78]. However, the importance of depth diminishes for tidal triggering, as 95% of seismic energy release occurs in the shallow crust (0–50 km), where horizontal shear stresses dominate earthquake generation processes [78]. This indicates that while tidal stresses increase with depth, their role in earthquake triggering is largely confined to shallower depths.

Further, the varying periods of tidal loading, also known as the tidal constituents, are the greatest during the diurnal and semi-diurnal cycles [79]. The periodic stress perturbations due to tidal cycles reveal that, under certain conditions, stress amplitude can be significantly lower or higher during alternate low- and high-amplitude tidal cycles. This can be observed at alternate low- and high-amplitude semidiurnal cycles, appearing at a diurnal period [7]. Also, it has been observed that the amplitude of the tidal cycles varies at different geographical regions around the globe, which has been extensively explored using satellite altimeter data from Topex/Poseidon [80]. Depending upon the compressional/extensional tidal force, the fluid diffusion can explain the permeability structure and associated mechanism and pathway of fluid circulations in the system (Figure 10).

2.6. Implications from the External Modulations of the Fluid Dynamics

The careful review of the literature not only sheds a light on the understanding of the endogenous dynamics of the magmatic systems but also on the modulation capabilities of the exogenous stress perturbing agents. It can be noted that the seasonal loads are the primary perturbation agents in case of continental land volcanoes, whereas the ocean tidal loadings are dominant in case of submarine magmatic systems (Figures 8 and 10). However notable contributions from both seasonal and tidal loadings can be observed on several volcanoes primarily on the coastal and fore-arc back-arc basins with notable presence of water bodies (Figure 8). One of the major examples is the Campi Flegrei caldera, present at the coast of Sicily in Italy which receives a large amount of rainfall during the wet seasons and also a notable amount of tidal load from the Mediterranean Sea as well as the solid earth tides (Figure 11). This makes the system equally sensitive to both the external loads due to its special geographical locations. Various studies on the unrest volcano have revealed that the volcano tectonic events are largely modulated by the seasonal pore-pressure change from the rainfall and tidal loading [8, 31]. On a specific note, the differential observations were noted during the different rates of inflation of the magmatic system which is under an evolution of the inflation stage producing an elevated number of seismic events with time [31] (Figure 11).

To quantitatively describe the evolving deformation behavior of the magmatic system for our specific case study at the Campi Felgrei Caldera, Italy, we classify the observed inflation trends into two/three categories:

- **Slower Rate of Inflation (SRI):** periods characterized by gradual uplift or pressurization within the magma or hydrothermal reservoir, typically associated with lower fluid injection rates and limited deformation acceleration.

- **Higher or Accelerated Rate of Inflation (HRI/ARI):** intervals marked by rapid increases in deformation rate, reservoir pressurization, or fluid accumulation, often preceding enhanced unrest or micro-seismic activity.

This distinction allows for better assessment of the magmatic system's sensitivity to external perturbations, as external stressors such as rainfall or tidal loading may influence the system differently under varying inflation regimes.

It was observed that during the slower rate of inflation period (SRI) the pore-pressure change due to seasonal rainfall was able to modulate the deformation but with further evolution with the rate of inflation and accumulation of further more fluids in the hydrothermal system made the system sensitive to tidal loadings during the Higher/Accelerated rates of inflation periods (HRI/ARI) (Figure 12). Therefore, it was presumed that by observing the natural agent of external stress perturbing agent for the modulated events, the associated stress of stress of the magmatic system can be estimated [31] (Figure 12).

The shift from rainfall- to tide- dominant modulation with increasing inflation rate reflects a transition toward a critically pressurized magmatic–hydrothermal system. During the Slower Rate of Inflation (SRI) phase, higher permeability allows rainfall- driven hydrological loading to influence shallow stress and fluid flow. As inflation accelerates to the Higher or Accelerated Rate of Inflation (HRI/ARI) phase, rising overpressure seals fractures and strengthens magma–crust coupling, reducing sensitivity to rainfall while enhancing response to small, coherent tidal stresses that penetrate the full crustal column. This can be observed in the declustered events which were specifically the volcano tectonic events caused due to the fracture failures [31]. The ARI threshold marks this transition and is defined by a nonlinear acceleration in uplift or deformation rate—typically an order of magnitude above SRI—accompanied by intensified micro-seismicity and gas-flux variations, indicating that tidal forcing has become the dominant modulating process.

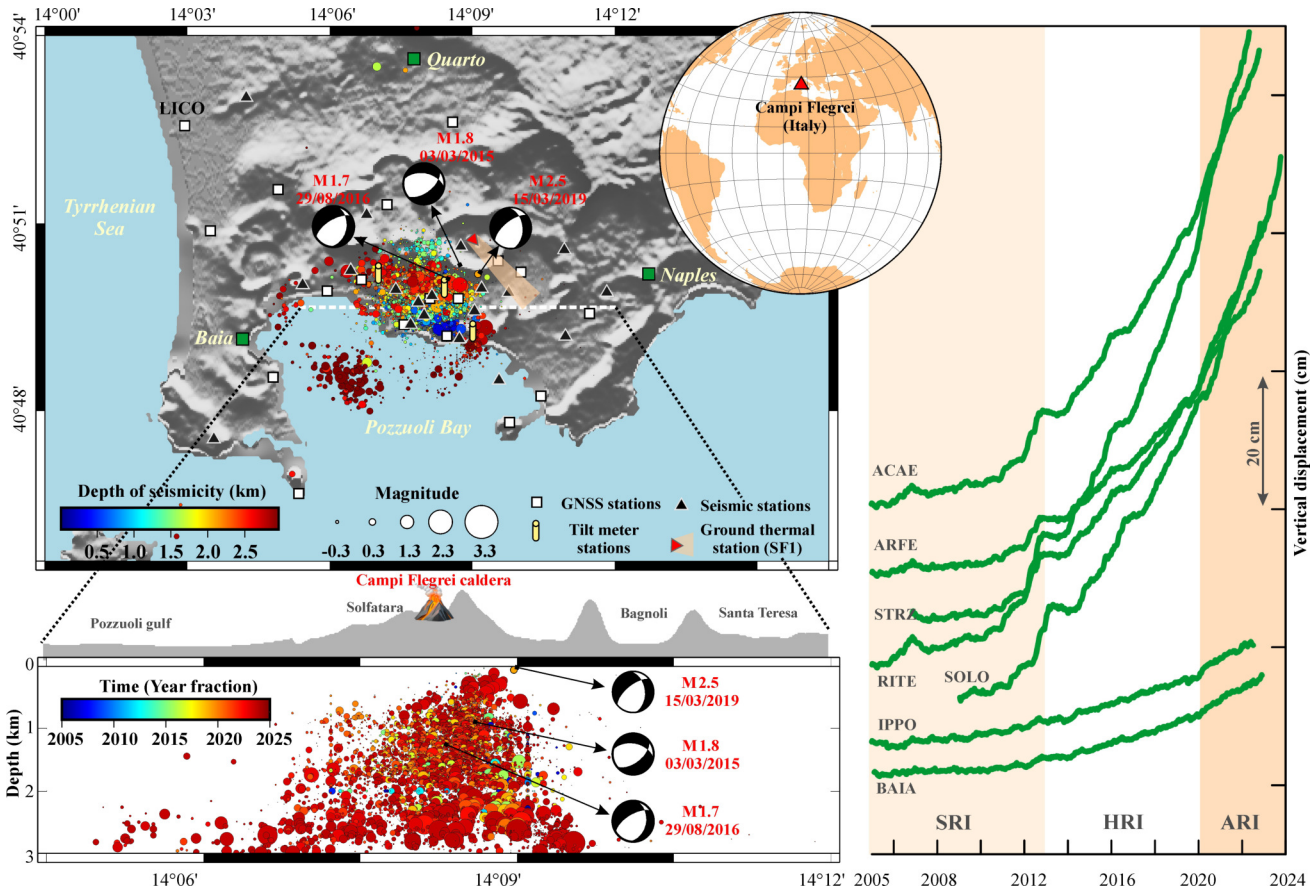

Figure 11. General Morphology, Seismicity and GNSS observations at the Campi Flegrei caldera, Italy. Globe inset shows the region of Campi Flegrei Caldera. Top panel: White rectangles are the GNSS stations. Black triangles mark the location of Seismic stations. Seismicity is shown in color size scale as represented along with fault plane solution of random events. Bottom panel: Seismicity with respect to depth along with fault plane solution of random events is shown at the respective cross-section (white dashed line in upper panel). Right panel: The vertical displacements observed in the region at different GNSS stations (Modified after [31]).

3. Monitoring of Magmatic Systems, External Forcing and Scientific Advancement: A Chronological Observation

For the contribution towards precise hazard estimation and possible mitigation, volcano monitoring plays a vital role, which has been rapidly evolving since the satellite era. After the improvement of geodetic and other geophysical techniques combined with statistical methods and historical datasets, several reports have focused on the working of volcanic and hydrothermal systems through complex internal processes of magma movement, as well as the dynamic structure of the system and associated failure mechanisms in the last two decades (Table 2). With accurate measurements, the eruption cycles and associated fault dynamics were also neatly explored in the last two decades which has vastly improved the understanding of the eruption mechanisms at different volcanoes such as basaltic, shield, sub-marine, aerial and stratovolcanoes around the globe (Table 3). In addition to that, the effect of natural external forces on the deformation processes was recognized centuries ago. Still, due to the advancements in geodetic and seismic monitoring in recent decades, the possibility of an accurate estimation of the fluid accumulation and mode, as well as the size of the eruption in the case of volcanoes and the permeability structure along with the fluid pathways in the case of hydrothermal systems, has been well explored. The apparent seasonality in global eruption occurrence is unlikely to be a mere reporting artifact; rather, it reflects a physically consistent response of near-critical volcanic systems to seasonal surface-loading cycles. Continued improvement in long-term, high-resolution monitoring networks will be essential to better quantify these interactions and distinguish genuine physical modulation from residual observational bias.

The fluid mechanics associated with the deformations have also been sufficiently explored, including the effect of exogenous forces (Table 4). However, the complex magma chamber and caldera dynamics during the evolution of the magmatic system in different stages of an eruption cycle and the feedback mechanism between the externally acting natural forces and the internal processes during the varying complex dynamics during different stages have not been well explored. Also, the external loadings in a spatial and temporal context following the geographical and

depth variance of the tidal loading are combined with several tidal constituents of varying amplitudes, generating varying mechanisms of tidal modulations that are not explored (Table 5). The tabular section has been divided into four segments; the first segment is focused on the volcanic deformation observation and modeling techniques for hazard estimation and mitigation (Table 2), followed by a segment focused on the eruption cycles and associated complex caldera dynamics (Table 3). Further, the segments are focused on rainfall and seasonal cycles modulating volcanic activity (Table 4), and a segment is focused on hydrothermal systems associated with tectonic environments and related seismicity dominated by tidal loadings later on (Table 5).

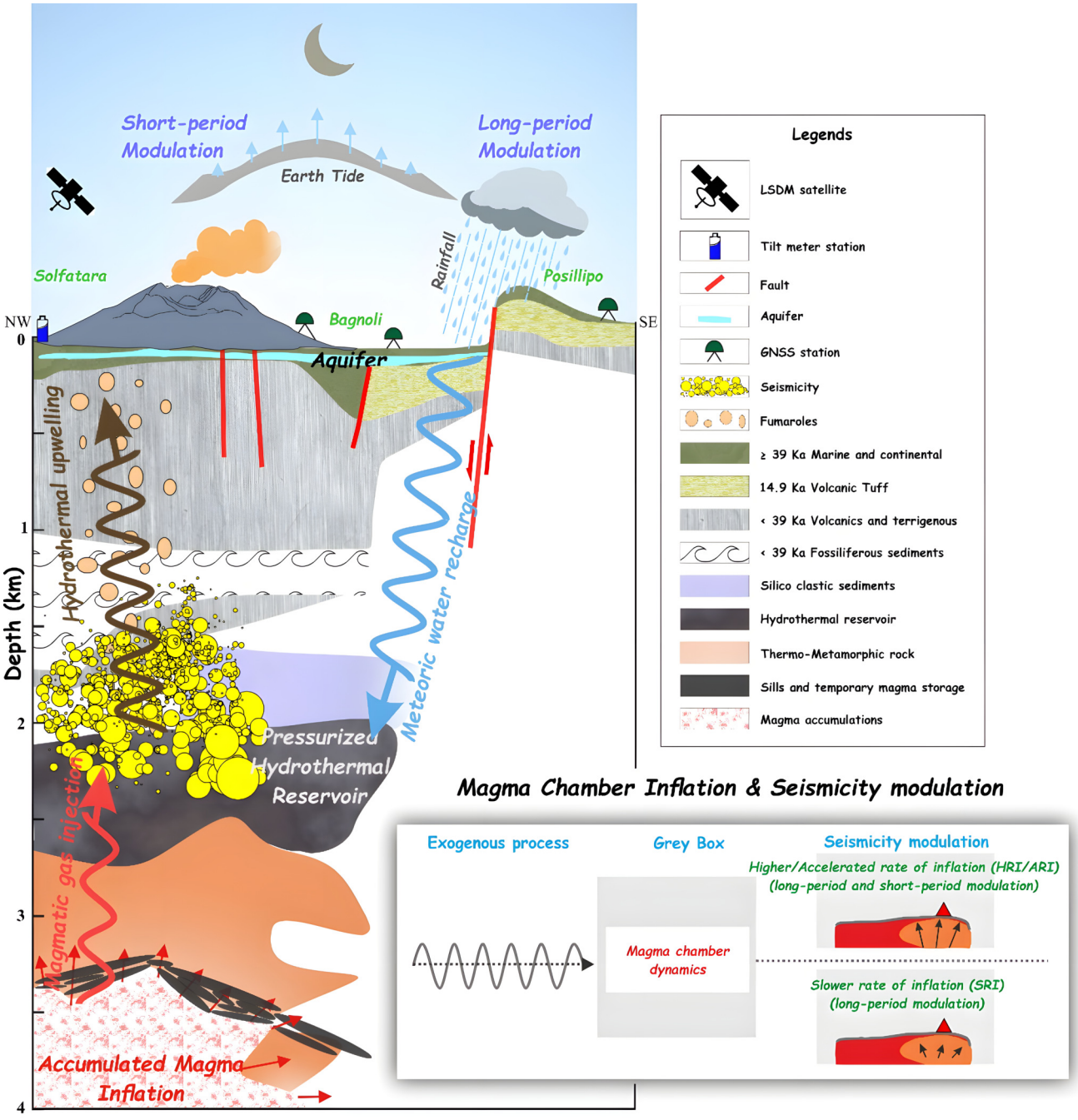

Figure 12. Schematic representation of different exogenous processes (Short-period tidal stress and Long-period seasonal load) acting on the Campi Flegrei caldera and associated lithology, different features such as fault planes with a cross-sectional view. Inset shows the representation of possible mechanism of short- and long-period exogenous processes for seismicity modulation during SRI (slower rate of inflation) and HRI (Higher rate of inflation) and ARI (higher rate of inflation). During HRI and ARI the higher inflation rate due to higher displacements can generate both long-period and short-period modulation whereas in case of SRI the lower displacements and lower inflation rate can only generate long-period modulations (Modified after [31]).

Table 2. Information on monitoring of volcanic deformations and source modelling of the sub-surface conditions compiled from several contributions [15, 81–84].

Focus/Region	Key Findings	Implications
Kīlauea and Mauna Loa (Hawaii)	Ground-based volcano deformation monitoring; links surface deformation to subsurface magma dynamics.	Provides insights into surface deformation dynamics and its relation to volcanic processes.
Long Valley Caldera (California)	Used InSAR to model magma movement and estimate magma chamber geometry and pressure changes.	Advances understanding of magma chamber processes and deformation patterns.
South American volcanoes	Demonstrated the utility of satellite radar for detecting undocumented deformation across South America.	Shows the potential of satellite radar in identifying deformation in remote regions.
Mount St. Helens (USA), Yellowstone (USA)	Comprehensive review of GNSS, InSAR, and leveling techniques for magma chamber monitoring.	Highlights the integration of various geodetic methods for detailed magma dynamics study.
Bárðarbunga-Holuhraun (Iceland)	Combined InSAR, GNSS, and seismic data to track magma dynamics, including dike propagation and caldera subsidence.	Provides real-time monitoring techniques for volcanic eruption forecasting.
Various global examples	Reviewed new technologies such as UAVs and machine learning in volcano deformation monitoring.	Explores cutting-edge technologies to improve eruption prediction and monitoring.
Kīlauea (Hawaii), Mount Etna (Italy)	Developed simple elastic models for magma chamber deformation, estimating depth and volume changes.	Early models for estimating magma chamber properties using surface deformation.
Widely applied in GNSS and InSAR studies	Analytical solutions for surface deformation due to shear and tensile faults, particularly for dike intrusions.	Critical for modeling deformation in volcanic systems with active dikes.
General magma reservoirs	Examined crustal loading on magma chamber evolution; integrated Mogi and Okada models with crustal interactions.	Improves understanding of how crustal loading affects magma chamber dynamics.
Volcanic systems with shallow magma sills	Modeled shallow magmatic sill inflation using InSAR and finite element methods.	Advances the modeling of shallow magmatic systems and their deformation.
Various volcanic and tectonic regions	Introduced numerical approaches for modeling complex geodetic signals from earthquakes and volcanoes.	Provides more accurate models for deformation in complex tectonic environments.
General volcanic settings	Demonstrated the importance of crustal heterogeneities in improving magma chamber models using finite element methods.	Highlights the need to account for crustal variations in deformation models.
Yellowstone (USA), Campi Flegrei (Italy)	Developed d-MODEL MATLAB toolbox for geodetic inversion, integrating multiple deformation models.	Provides tools for better interpreting geodetic data in volcanic areas.
Mount Etna (Italy)	Introduced a genetic algorithm for inversion of elastic deformation models.	Offers a new method for handling complex volcanic environments and multi-dataset integration.
Campi Felgrei (Italy)	Monitored different rates of inflation periods and tracked the associated fluid, pressure and depth change in the source	Provided insights into the endogeneous changes in the different periods of inflation

Table 3. Some of the most important contributions towards understanding of Eruption cycles and caldera dynamics associated with the magmatic system [27, 33, 34, 36].

Focus/Region	Key Findings	Implications
Silicic volcanoes	Eruption cycles involve stages of inflation, eruption, and repose caused by stick-slip behavior and Newtonian flow.	Explains eruption dynamics as cyclic behavior due to interactions between magma flow and conduit wall.
Shallow magma conduit	Cyclic eruption patterns arise from pressure buildup and plug recrystallization, with non-linear magma flow altering conduit dimensions.	Highlights mechanisms of pressure changes and plug dynamics affecting eruption cycles.
Geophysical monitoring methods	Ground deformation patterns can be analyzed using combined geodetic techniques like InSAR and GNSS surveys.	Long-term monitoring provides insights into inflation rates and magma dynamics during eruption cycles.
Icelandic volcanoes	Eruption cycles include inflation, intrusion, and eruption, with geodetic data revealing magma movement constraints.	Integration of seismic and deformation data enhances understanding of volcanic activity.
Caldera ring faults	Ring faults evolve through 4 stages during collapse, influenced by subsidence, stress conditions, and structural characteristics.	Provides structural insights into caldera formation and fault dynamics during eruption stages.
Conduit processes	Time-varying conduit processes and geometry affect magma ascent, strain, and decompression rates.	Emphasizes the role of conduit shape and boundary conditions in influencing eruption styles and cycles.
Juan de Fuca ridge, Northeast Pacific	Reactivation of outward-dipping ring faults during inflation/deflation with distinct seismic patterns.	Demonstrates fault reactivation and seismic activity's link to magma chamber dynamics.
Eruption cycles and deformation	Timescales of eruption cycles depend on material properties, conduit features, and non-linear magma movement.	Identifies factors controlling the duration of eruption cycles and their variability.
Juan de Fuca ridge, Northeast Pacific	State of Stress during different stages and susceptibility to triggering from tidal loads during critical inflation in Pre-eruption period	Probability of estimating the eruption and forecast using triggering susceptibility of events

4. Summary

Volcano monitoring relies on geodetic techniques like InSAR, GNSS, and leveling to track surface deformation and infer magma dynamics. Early studies, introduced InSAR for precise monitoring, while Dvorak and Dzurisin [85] highlighted the use of ground-based methods. Advances by Wicks et al. [86] and Sigmundsson et al. [40] integrated multi-disciplinary data for real-time insights. Numerical models, starting with Mogi [81] and Okada [82], provided foundational frameworks for understanding deformation. Enhancements by Battaglia et al. [84] introduced tools like d-MODEL and GAME for robust geodetic inversions. Eruption cycles involve inflation, eruption, and repose, as explored by Denlinger and Hoblitt [35], and Sahoo et al. [31], with caldera dynamics shaped by ring faults [34]. Comprehensive geophysical monitoring, reviewed by Dzurisin and Lisowski [83], improves hazard assessments, while studies of conduit dynamics [25] elucidate eruption variability. The deformation monitoring at the magmatic systems around the globe has rapidly evolved, but the different stages of accelerating deformation through combined geodetic modelling methods have not been explored in-detail at particular volcanoes with higher volcanic hazards due to large population inhabitation.

Table 4. Available information on understanding the Effect of exogenous forces on volcanic activity and associated fluid flow from dedicated contributions [12, 38–40, 53, 55, 58, 78, 79].

Focus/Region	Key Findings	Implications
Klyuchevskoy Volcano	Spring snowmelt infiltration increases pore pressure, promoting seismicity or eruptions. Highlights hydrology's role in volcanic activity.	Seasonal hydrology directly impacts volcanic activity; monitoring snowmelt can enhance eruption forecasting.
Mount Rainier	Seasonal snow loading impacts volcanic systems. Winter snow accumulation increases stress; spring snowmelt reduces load, inducing seismicity.	Accounting for seasonal stress variations can improve hazard management and long-term eruption prediction models.
Global (300 years data)	Seasonal volcanic eruption patterns linked to hydrological cycles and stress changes, particularly for smaller eruptions (VEI 0–2).	Seasonal patterns in eruptions underline the need for integrating climatic cycles into volcanic hazard models, especially for smaller eruptions.
Mount Ruapehu	Seasonal snowmelt infiltrates hydrothermal systems, triggering phreatic explosions. Emphasizes hydrological inputs in volcanic risk management.	Understanding snowmelt dynamics is critical for hazard planning in snow-dominated volcanic regions.
Icelandic volcanic systems	Deglaciation reduces surface pressure, enhancing mantle melting and magma generation, leading to increased volcanic activity.	Accelerated glacier melting due to climate change could increase volcanic activity in glacial regions.
Kermadec Arc	Glacial periods correlate with increased eruptions due to reduced hydrostatic pressure destabilizing magma chambers.	Sea level fluctuations must be considered in assessing volcanic hazards for submarine and coastal volcanoes.
Yellowstone Caldera	Snowmelt alters subsurface fluid pressures, influencing seismicity and geothermal activity. Highlights the role of snow-driven hydrological changes in volcanic systems.	Snowmelt-driven hydrological changes should be integrated into geothermal monitoring and eruption forecasting strategies.
Mid-ocean ridge volcanism	Lower sea levels during glacial periods increase magma flux and eruption rates. High sea levels during interglacial periods suppress magmatic activity.	Long-term sea level changes significantly influence magma dynamics, necessitating their inclusion in models of mid-ocean ridge volcanic activity.
Santorini Caldera	Lower sea levels during glacial periods reduce hydrostatic pressure, increasing eruption frequency and magnitude. Higher sea levels suppress volcanic activity.	Sea level changes, influenced by climate cycles, play a crucial role in modulating volcanic hazards for island arc systems.
Katla Volcano	Seasonal snow and glacier meltwater modulate hydrothermal systems, triggering seismic unrest. Highlights the role of glacial dynamics in high-latitude volcanic behavior.	Glacier dynamics need to be closely monitored to predict seismic and volcanic activity in high-latitude regions.
Aleutian Arc	Sea level changes and glacial melting reduce stabilizing pressure on magma chambers, increasing eruption potential, especially in subglacial and submarine systems.	Dual impact of sea level and glacial changes should be factored into volcanic hazard assessments in subglacial and marine environments.
Magma cooling model	Modeled magma cooling and gas pressure buildup in spherical magma chambers. Eruptions occur when overpressure surpasses twice the rock's tensile strength.	Magma chamber pressure evolution models aid in understanding long repose periods and eruption triggers.
Rainfall and eruptions	Rainfall infiltration initially constrains eruptions by increasing the burden on volcanoes but can trigger eruptions when the system nears critical parameters.	Rainfall patterns must be included in volcanic monitoring as they can delay or trigger eruptions under critical conditions.

Table 4. *Cont.*

Focus/Region	Key Findings	Implications
Rainfall and dome collapse	Persistent heavy rainfall (15 mm/hr for 2–3 hr) can cause dome collapse in critical states, though most heavy rainfall events do not result in volcanic activity.	Rainfall-triggered dome collapse should be considered in hazard assessments, especially during prolonged rainfall events.
Rainfall-induced seismicity	Rainfall increases pore fluid pressure, reducing fault strength and triggering earthquakes down to 4 km depth.	Rainfall's effect on seismicity needs to be factored into earthquake hazard assessments in volcanic regions.
Pore fluid pressure	High pore pressure reduces effective rock pressure, facilitating fractures and embrittlement, even in compacted zones.	High pore pressure in volcanic structures could serve as an early warning signal for potential eruptions or intrusions.
Pore fluid overpressure	Pore fluid pressure is the dominant factor influencing the overpressure needed to trigger fractures and volcanic activity.	Variability in pore fluid pressure could provide insights into eruption thresholds and magma chamber stability.
Kīlauea, Hawaii	Rain-induced pore pressure changes weakened volcanic structure, leading to collapse, dyke intrusion, and eruption without significant summit inflation.	Rain-triggered collapses should be accounted for in volcanic hazard models, particularly in regions experiencing increased rainfall due to climate change.
Tidal periodicity in earthquakes	Identified fortnightly tidal frequencies in seismic events using Fourier spectrum analysis.	Tidal influences on seismic activity can provide insights into periodic stress variations affecting volcanic regions.
Tidal triggering of eruptions	Longer-period tidal cycles with higher stress amplitudes can trigger volcanic eruptions.	Tidal cycles could help predict volcanic activity by identifying stress peaks associated with gravitational forces.
St. Helens (pre-eruption swarms)	Identified tidally modulated seismic swarms with higher b-values, suggesting fluid-dominated failure mechanisms linked to ocean tidal loading.	Ocean tidal loading should be considered when interpreting pre-eruption seismic swarms, especially in fluid-dominated systems.
Campi Flegrei caldera	Solid Earth tidal loading did not trigger pre-eruption seismic events. Tidal triggering depends on magma chamber inflation state.	Tidal effects on volcanic activity are conditional and require critical magma chamber inflation, emphasizing the need for integrated geophysical monitoring.
Tidal stress computation	Developed a program for precise tidal loading computations (gravity, strain, tilt) using regional/global models and Green's functions.	Advanced tidal loading models provide accurate tools for assessing tidal impacts on volcanoes and seismic zones globally.
Ocean tidal loading (Japan)	Improved ocean tidal load calculations with fine-scaled grids for accurate estimations, including multi-annual long-period tides.	High-resolution tidal load models enhance regional predictions of stress variations on volcanic and seismic systems.
Tides and geological systems	Linked tidal forces to volcanic and seismic activity through orbital cycles (e.g., Milankovitch cycles), suggesting tides' impact on magma chambers and crustal stress.	Long-term orbital cycles may explain periodic geological changes, highlighting the interplay between celestial mechanics and Earth's volcanic and tectonic processes.
Mount Etna, Italy	Effect of rainfall and pore-pressure change in destabilization of pre-existing fracture pathways for fluid transfer	Rainfall and associated pore pressure change can destabilize fluid pathways and promote eruptions

Table 5. Information on the understanding of fluid transfer and associated deformations in the continental as well as submarine hydrothermal systems [4, 7, 43, 61, 71, 76, 77, 87].

Focus/Region	Key Findings	Implications
Seismic swarms in the East African Rift system	Magmatic fluid intrusions generate overpressure, reducing fault strength and triggering seismicity.	Demonstrates the role of fluid dynamics in seismic swarms within extensional tectonic settings such as rift zones.
Seismic swarms in the Cascadia Subduction Zone	Low-frequency earthquakes and tremors linked to transient fluid pressure pulses from slab dehydration.	Highlights fluid overpressure as a primary driver of seismicity in hydrothermal systems within subduction environments.
Fluid migration and seismic swarms in the Nankai Subduction Zone	Transient fluid pulses within faults are closely associated with low-frequency tremors, providing insights into fluid-induced seismicity in hydrothermal systems.	Advances understanding of seismicity driven by fluid migration in subduction zones.
Fault-valve model and fluid-driven seismicity	Episodic fluid pulses reduce effective stress, enabling shear slip and localized seismic swarms.	Foundational model for transient fluid-driven seismicity in transform fault systems like the San Andreas Fault.
Seismic swarms in Yellowstone's volcanic hydrothermal system	Seismic swarms are driven by pressurization and migration of hydrothermal fluids in shallow crustal layers rather than direct magmatic intrusion.	Highlights the role of fluid pressurization in driving seismicity in volcanic hydrothermal systems.
Pre-eruption swarms at Mount Ontake, Japan	Upward migration of supercritical fluids through fractures triggers seismic swarms before phreatic eruptions.	Demonstrates the role of fluid dynamics in triggering seismicity before explosive hydrothermal events.
Static stress transfer in earthquake triggering	Minimal stress changes can accumulate to trigger fault slip, challenging the idea of a critical stress level.	Emphasizes the sensitivity of fault systems to subtle stress changes and cumulative triggering dynamics.
Hydrothermal earthquakes in oceanic crust	Tidal forces influence micro-seismicity in regions of high tectonic stress, though tidal stress alone doesn't generate earthquakes.	Suggests complex interplay of oceanic and Earth tides with fluid movement near submarine hydrothermal systems.
Tidal stress effects on seismicity	Tidal triggering is influenced by stress state, failure depth, and tidal loading amplitude ($\sim$0.003 MPa), with shallow faults favoring extensional stress conditions.	Provides a detailed picture of tidal stress modulation in seismic events, with spatial variations based on fault geometry and depth.
Ocean tidal load effects on hydrothermal systems	Micro-seismicity triggered by low tides, with tidal effects driven by normal stress changes imparted by ocean tides.	Demonstrates tidal modulation of seismicity in oceanic hydrothermal systems and mid-ocean ridges.
Tidal triggering at East Pacific Rise	Tidal triggering depends on fault geometry and magma chamber dynamics, with high tides compressing chambers and triggering seismicity.	Provides insights into the interplay between tidal forces and magma chamber behavior in mid-ocean ridge systems.
Tidal sensitivity at Juan de Fuca Ridge	Tidal loading correlates with magma chamber inflation/deflation, imparting Coulomb stress on caldera ring faults.	Highlights complex tidal effects on submarine volcanic systems, including opposing stress impacts during different eruption periods.
Tidal stresses and deep-focus earthquakes	Tidal stresses peak at $\sim$900–1500 km depth but are smaller at depths where most seismic energy is released. Radial stresses parallel to Earth's surface are the most likely contributors to seismicity.	Explores tidal stress contributions to seismic activity, emphasizing variations with depth and geography.
Crust mantle transition zone at Transform fault	High amplitude tidal loading during diurnal and fortnightly periods can be more effective at deeper depths for tidal triggering process	Shows that there are some spatio temporal conditions on which the triggering process is dependant

Several studies have investigated how climatic and tidal factors influence volcanic activity. Seasonal cycles like snowmelt and rainfall can significantly influence volcanic eruptions by altering pore pressure, surface stress, and hydrothermal systems. For example, Fedotov et al. [55] documented the impact of spring snowmelt on Klyuchevskoy Volcano, while Moran et al. [53] reported the effects of snow loading and melt on Mount St. Helens. Sea level changes associated with glacial cycles can impact magma generation, chamber stability, and eruption frequency. Sigmundsson et al. [40] examined the impact of deglaciation and sea level changes on Icelandic volcanic systems, and Watt et al. [52] analyzed the influence of sea level fluctuations on the Kermadec Arc. Tidal forces can trigger seismic activity and potentially eruptions, especially in systems already near critical stress levels. McNutt and Beavan [30] worked on the swarm of seismic events in the pre-eruption period of the volcanic eruption at St. Helens and reported that the group of events had different characteristics. Agnew [79] greatly impacted the correlation of tidal stress with different events by providing a program for the computation of tidal loading. Although the mechanisms involved in the sensitivity of the volcanic system to external natural forces during the different eruption cycles have already been explored, the complex interplay between the caldera dynamics during the cycles and associated deformation mechanisms triggered by the external forces has been poorly understood. During the pre-eruption stage, the magmatic system is most sensitive to periodic stress perturbations; however, the feedback response between external forces and internal dynamics during the evolution of the magmatic system's degree of inflation remains unexplored.

The contrasting behavior between volcanoes that erupt without measurable inflation and those that inflate without erupting is strongly influenced by the depth of the active reservoir and the relative dominance of magmatic versus hydrothermal processes. In deep-seated magmatic systems, pressure changes can be efficiently accommodated by ductile crustal deformation, resulting in minimal surface signals even when eruptions occur. Conversely, shallow, hydrothermally dominated systems can exhibit pronounced inflation due to vapor accumulation or pressurization of sealed aquifers without magma ascent to the surface. The degree of mechanical coupling between the reservoir and the surface, host-rock rheology, and the presence of interconnected fluid pathways largely determine whether deformation precedes eruption or remains aseismic and non-eruptive. Hence, the presence or absence of measurable inflation is not a universal predictor of eruption, but rather reflects system-specific depth, permeability, and coupling characteristics.

Research on fluid transfer and deformations in hydrothermal systems reveals the critical role of fluid dynamics in seismic activity across various tectonic settings. Keir et al. [71] and Husen et al. [72] linked seismic swarms in rift zones and volcanic systems to magmatic and hydrothermal fluid pressurization. Obara & Kato [61] demonstrated the role of transient fluid pulses in subduction zones, while fault-valve model highlighted episodic fluid-induced slip in transform faults. Tidal influences on hydrothermal systems were explored by Wilcock et al. [7] and Scholz et al. [88], demonstrating the impact of tidal loading on microseismicity in submarine environments, with variations dependent on fault geometry and depth. Advances in geodetic techniques have improved the monitoring of deformation associated with fluid migration. These studies highlight the complex interplay between fluids, tectonics, and external forces, such as tides, in driving hydrothermal seismic phenomena. Furthermore, the threshold of loading stress has reportedly been avoided for tidal modulation of seismicity at hydrothermal systems [87]; however, the role of spatial and temporal conditions in the interaction between fluid circulation and tidal loading remains unexplored. Further, the 2022 Hunga Tonga–Hunga Ha'apai eruption demonstrates the bidirectional coupling between magmatic and atmospheric systems, where external pressure variations and eruption-driven atmospheric waves can transiently modulate stress and energy release across the solid Earth system.

Adding to that, historical eruption databases are recorded, but the effects of climate change through the quantitative effect of rainwater infiltration, which can be accurately estimated, have not been explored in the context of increased rainfall due to climate change. Due to change in temperature and snow caps the associated load can increase/decrease on the magmatic system which further can modulate the system. Increased inhabitations around the active volcanoes have not only increased the associated hazards to the growing population but also the urbanizations around the systems also disrupts the natural climatic components and changes various patterns that can impact the magmatic systems. With this evolution keeping in mind, further studies towards the combined effects should be carried out for a better estimation of the associated hazards and possible mitigations.

Therefore, the feedback response between the different prominent external stress perturbing forces like rainfall and tidal loading on the highly sensitive and fluid-dominated critical state volcanic and hydrothermal systems must be explored to understand the sensitivity at different stages to different forces and associated mechanisms in the spatio-temporal context in the complex magmatic dynamics.

5. Future Perspectives

From the above summary and in-depth literature review the following future perspectives can be projected:

- Precise investigation of deformation patterns and associated mechanisms during unrest periods using combined geodetic and geophysical methods to understand magma chamber dynamics better, enabling more accurate hazard assessments and improved mitigation strategies.

- Analyzing the influence of external forces on caldera systems, with a specific focus on rainfall-induced pore pressure changes and tidal loading, to assess their impact on the current state of stress of the magmatic systems in the direction of eruption forecast and hazard estimation.
- Exploration of the complex dynamics of caldera systems during various stages of the eruption cycle, along with their sensitivity to external forces, will help to develop a clearer understanding of the state of stress during different phases of magmatic systems.
- Investigation of the effects of seasonal cycles on historical volcanic eruption records is needed to evaluate how the climatic forces may influence caldera structures, offering insights into the potential role of global climate change and especially the intensified rainfall on future volcanic activity.
- Deep exploration of the hydrothermal systems with advanced seafloor geodesy and geophysical methods is required to understand fluid transfer mechanisms across different tectonic settings, focusing on seismic swarm patterns and spatio-temporal parameters in tidal triggering processes.

Author Contributions

B.K. provided research ideas. S.S. performed all the analysis, wrote the original draft. B.K., reviewed & edited the draft and interpreted the results. Both the authors contributed equally and took part in finalizing the manuscript.

Funding

This research received no external funding.

Institutional Review Board Statement

Not applicable.

Informed Consent Statement

Not applicable.

Data Availability Statement

All datasets shown in this work are presented in the respective articles containing the public archive information.

Acknowledgments

This work has been performed within the framework of Sambit Sahoo's Ph.D. thesis at NIT Rourkela under the supervision of Bhaskar Kundu S.S. was supported by CSIR-UGC fellowship during this work and currently supported by SEESHA project funded by Department of Space (DOS), Indian Space Research Organization (ISRO). We would like to thank M. Santosh for inviting us to contribute to the esteemed journal. We would also like to thank Simona Petrosino (National Institute of Geophysics and Volcanology, Italy), Amanda Thomas (University of Oregon, USA), William Wilcock (School of Oceanography, USA), Vaklav M. Kuna (Insitute of Geophysics, Czech republic), Denis Legrand (UNAM, Mexico), Rajeev Kumar Yadav (NGRI, Hyderabad), Abhijit Ghosh (University of California Riverside, USA), Roland Bürgmann (University of California, Berkeley), and Shuanggen Jin (Chinese Academy of Sciences, China) for the help in diverse datasets archive, technicality in analysis and their constructive comments during timeframe of Ph.D. thesis at NIT Rourkela, which ultimately improved the quality of the present review work. We are also thankful to the two anonymous reviewers, M. Santosh and Anilkumar Y. for providing their constructive comments which has also improved the quality of the manuscript.

Conflicts of Interest

The authors declare that they have no known competing financial interests or personal relationships that could have appeared to influence the work reported in this paper.

Use of AI and AI-assisted Technologies

During the preparation of this work, the authors used Grammarly English correction Tool. After that, the authors reviewed and edited the content as needed and take full responsibility for the content of the publication.

References

1. Caricchi, L.; Townsend, M.; Chaillou, E.; et al. Volcanic eruptions and their impact on human settlements: A review of key processes and implications. *J. Volcanol. Geotherm. Res.* **2021**, *417*, 107–128. https://doi.org/10.1038/s43017-021-00174-8
2. Townsend, M.; Huber, C. A critical magma chamber size for volcanic eruptions. *Geology* **2020**, *48*, 431–435. https://doi.org/10.1130/G47045
3. Lejeune, A.M.; Richet, P. Rheology of crystal-bearing silicate melts: An experimental study at high temperatures and pressures. *J. Geophys. Res. Solid Earth* **1995**, *100*, 4215–4229. https://doi.org/10.1029/94JB02986
4. Glasby, G.P.; Kasahara, J. Influence of tidal effects on the periodicity of earthquake activity in diverse geological settings with particular emphasis on submarine hydrothermal systems. *Earth Sci. Rev.* **2001**, *52*, 261–297. https://doi.org/10.1016/S0012-8252(00)00031-3
5. Gregg, P.M.; Le Mével, H.; Zhan, Y.; et al. Stress triggering of the 2005 eruption of Sierra Negra volcano, Galápagos. *Geophys. Res. Lett.* **2018**, *45*, 13288–13296. https://doi.org/10.1029/2018GL080393
6. Loughlin, S.C.; Sparks, R.S.J.; Brown, S.K.; et al. *Global Volcanic Hazards and Risk*; Cambridge University Press: Cambridge, London, UK, 2015. https://doi.org/10.1017/CBO9781316276273
7. Wilcock, W.S.; Tolstoy, M.; Waldhauser, F.; et al. Seismic constraints on caldera dynamics from the 2015 Axial Seamount eruption. *Science* **2016**, *354*, 1395–1399. https://doi.org/10.1126/science.aah5563
8. Petrosino, S.; Cusano, P.; Madonia, P. Tidal and hydrological periodicities of seismicity reveal new risk scenarios at Campi Flegrei caldera. *Sci. Rep.* **2018**, *8*, 31760. https://doi.org/10.1038/s41598-018-31760-4
9. Niu, J.; Song, T.R.A. Response of repetitive very-long-period seis-

mic signals at Aso Volcano to periodic loading. *Geophys. Res. Lett.* **2021**, *48*, e2021GL092728. https://doi.org/10.1029/2021GL092728

10. Dumont, S.; Petrosino, S.; Neves, M.C. On the link between global volcanic activity and global mean sea level. *Front. Earth Sci.* **2022**, *10*, 845511. https://doi.org/10.3389/feart.2022.845511
11. Farquharson, J.I.; Amelung, F. Extreme rainfall triggered the 2018 rift eruption at Kīlauea Volcano. *Nature* **2020**, *580*, 491–495. https://doi.org/10.1038/s41586-020-2172-5
12. Sottili, G.; Lambert, S.; Palladino, D.M. Tides and volcanoes: A historical perspective. *Front. Earth Sci.* **2021**, *9*, 777548. https://doi.org/10.3389/feart.2021.777548
13. Auker, M.R.; Sparks, R.S.J.; Siebert, L.; et al. A statistical analysis of the global historical volcanic fatalities record. *J. Appl. Volcanol.* **2013**, *2*, 2. https://doi.org/10.1186/2191-5040-2-2
14. Pyle, D.M.; Barclay, J. Historical records of volcanic eruptions deserve more attention. *Nat. Rev. Earth Environ.* **2020**, *1*, 183–184. https://doi.org/10.1038/s43017-020-0044-z
15. Segall, P. *Earthquake and Volcano Deformation*; Princeton University Press: Princeton, NJ, USA, 2010. https://doi.org/10.1515/9781400833856
16. Venzke, E.; Sennert, S.K.; Wunderman, R. Reports from the Smithsonian's Global Volcanism Network, February 2008. *Bull. Volcanol.* **2009**, *71*, 113–115. https://doi.org/10.1007/s00445-008-0221-2
17. Ryan, M.P. Mechanics and three-dimensional internal structure of active magmatic systems: Kīlauea Volcano. *J. Geophys. Res. Solid Earth* **1988**, *93*, 4213–4248. https://doi.org/10.1029/JB093iB05p04213
18. Taisne, B.; Tait, S. Effect of solidification on a propagating dike. *J. Geophys. Res. Solid Earth* **2011**, *116*, B01206. https://doi.org/10.1029/2009JB007058
19. Annen, C.; Blundy, J.D.; Sparks, R.S.J. The genesis of intermediate and silicic magmas in deep crustal hot zones. *J. Petrol.* **2006**, *47*, 505–539. https://doi.org/10.1093/petrology/egi084
20. Fialko, Y.; Khazan, Y.; Simons, M. Deformation due to a pressurized horizontal circular crack in an elastic half-space. *Geophys. J. Int.* **2001**, *146*, 181–190. https://doi.org/10.1046/j.1365-246X.2001.00452.x
21. Cimarelli, C.; Costa, A.; Mueller, S.; et al. Rheology of magmas with bimodal crystal size and shape distributions: Insights from analog experiments. *Geochem. Geophys. Geosyst.* **2011**, *12*, Q07012. https://doi.org/10.1029/2011GC003606
22. Cashman, K.V.; Sparks, R.S.J. How volcanoes work: A 25-year perspective. *Geol. Soc. Am. Bull.* **2013**, *125*, 664–690. https://doi.org/10.1130/B30720.1
23. Neuberg, J.W.; Tuffen, H.; Collier, L.; et al. The trigger mechanism of low-frequency earthquakes on Montserrat. *J. Volcanol. Geotherm. Res.* **2006**, *153*, 37–50. https://doi.org/10.1016/j.jvolgeores.2005.08.008
24. Rivalta, E.; Dahm, T. Acceleration of buoyancy-driven fractures and magmatic dikes beneath the free surface. *Geophys. J. Int.* **2006**, *166*, 1424–1439. https://doi.org/10.1111/j.1365-246X.2006.02962.x
25. Gonnermann, H.M.; Manga, M. The fluid mechanics inside a volcano. *Annu. Rev. Fluid Mech.* **2007**, *39*, 321–356. https://doi.org/10.1146/annurev.fluid.39.050905.110207
26. Jellinek, A.M.; DePaolo, D.J. A model for the origin of large silicic magma chambers: Precursors of caldera-forming eruptions. *Bull. Volcanol.* **2003**, *65*, 363–381. https://doi.org/10.1007/s00445-003-0277-y
27. Sahoo, S.; Senapati, B.; Panda, D.; et al. Tidal triggering of micro-seismicity associated with caldera dynamics in the Juan de Fuca ridge. *J. Volcanol. Geotherm. Res.* **2021**, *417*, 107319. https://doi.org/10.1016/j.jvolgeores.2021.107319
28. Sparks, R.S.J.; Pinkerton, H.; Macdonald, R. The transport of xenoliths in magmas. *Earth Planet. Sci. Lett.* **1977**, *35*, 234–238. https://doi.org/10.1016/0012-821X%2877%2990126-1
29. Thomas, M.E.; Neuberg, J. What makes a volcano tick—A first explanation of deep multiple seismic sources in ascending magma. *Geology* **2012**, *40*, 351–354. https://doi.org/10.1130/G32868.1
30. McNutt, S.R.; Beavan, R.J. Eruptions of Pavlof volcano and their possible modulation by ocean load and tectonic stresses. *J. Geophys. Res. Solid Earth* **1987**, *92*, 11509–11523. https://doi.org/10.1029/JB092iB11p11509
31. Sahoo, S.; Kundu, B.; Petrosino, S.; et al. Feedback responses between endogenous and exogenous processes at Campi Flegrei caldera dynamics, Italy. *Bull. Volcanol.* **2024**, *86*, 22. https://doi.org/10.1007/s00445-024-01719-7
32. Jaupart, C.; Allègre, C.J. Gas content, eruption rate and instabilities of eruption regime in silicic volcanoes. *Earth Planet. Sci. Lett.* **1991**, *102*, 413–429. https://doi.org/10.1016/0012-821X(91)90032-D
33. Levy, S.; Bohnenstiehl, D.R.; Sprinkle, P.; et al. Mechanics of fault reactivation before, during, and after the 2015 eruption of Axial Seamount. *Geology* **2018**, *46*, 447–450. https://doi.org/10.1130/G39978.1
34. Acocella, V.; Di Lorenzo, R.; Newhall, C.; et al. An overview of recent (1988 to 2014) caldera unrest: Knowledge and perspectives. *Rev. Geophys.* **2015**, *53*, 896–955. https://doi.org/10.1002/2015RG000492
35. Denlinger, R.P.; Hoblitt, R.P. Cyclic eruptive behavior of silicic volcanoes. *Geology* **1999**, *27*, 459–462. https://doi.org/10.1130/0091-7613(1999)027<0459:CEBOSV>2.3.CO;2
36. Sturkell, E.; Einarsson, P.; Sigmundsson, F.; et al. Volcano geodesy and magma dynamics in Iceland. *J. Volcanol. Geotherm. Res.* **2006**, *150*, 14–34. https://doi.org/10.1016/j.jvolgeores.2005.07.010
37. Sahoo, S.; Tiwari, D.K.; Panda, D.; et al. Eruption cycles of Mount Etna triggered by seasonal climatic rainfall. *J. Geodyn.* **2022**, *149*, 101896. https://doi.org/10.1016/j.jog.2021.101896
38. Hainzl, S.; Kraft, T.; Wassermann, J.; et al. Evidence for rainfall-triggered earthquake activity. *Geophys. Res. Lett.* **2006**, *33*, L19303. https://doi.org/10.1029/2006GL027642
39. Mason, B.G.; Pyle, D.M.; Dade, W.B.; et al. Seasonality of volcanic eruptions. *J. Geophys. Res. Solid Earth* **2004**, *109*, B04204. https://doi.org/10.1029/2002JB002293
40. Sigmundsson, F.; Hooper, A.; Hreinsdóttir, S.; et al. Segmented lateral dyke growth in a rifting event at Bárðarbunga volcanic system, Iceland. *Nature* **2015**, *517*, 191–195. https://doi.org/10.1038/nature14111
41. Chiodini, G.; Caliro, S.; Avino, R.; et al. Hydrothermal pressure-temperature control on CO_2 emissions and seismicity at Campi Flegrei (Italy). *J. Volcanol. Geotherm. Res.* **2021**, *414*, 107245. https://doi.org/10.1016/j.jvolgeores.2021.107245
42. Lambert, S.; Sottili, G. Is there an influence of the pole tide on volcanism? Insights from Mount Etna recent activity. *Geophys. Res. Lett.* **2019**, *46*, 13730–13736. https://doi.org/10.1029/2019GL085525
43. Cochran, E.S.; Vidale, J.E.; Tanaka, S. Earth tides can trigger shallow thrust fault earthquakes. *Science* **2004**, *306*, 1164–1166. https://doi.org/10.1126/science.1103961
44. Lockner, D.A.; Beeler, N.M. Premonitory slip and tidal triggering of earthquakes. *J. Geophys. Res. Solid Earth* **1999**, *104*, 20133–20151. https://doi.org/10.1029/1999JB900205
45. Senapati, B.; Kundu, B.; Jin, S. Seismicity modulation by external stress perturbations in plate boundary vs. stable plate interior. *Geosci. Front.* **2022**, *13*, 101352. https://doi.org/10.1016/j.gsf.2021.101352
46. Emter, D. Tidal triggering of earthquakes and volcanic events. In *Tidal Phenomena*; Springer: Berlin, Germany, 1997; pp 293–309. https://doi.org/10.1007/BFb0011468
47. Marshall, L.R.; Maters, E.C.; Schmidt, A.; et al. Volcanic effects on

climate: Recent advances and future avenues. *Bull. Volcanol.* **2022**, *84*, 54. https://doi.org/10.1007/s00445-022-01559-3

48. Rampino, M.R.; Self, S.; Fairbridge, R.W. Can rapid climatic change cause volcanic eruptions? *Science* **1979**, *206*, 826–829. https://doi.org/10.1126/science.206.4420.826
49. Jull, M.; McKenzie, D. The effect of deglaciation on mantle melting beneath Iceland. *J. Geophys. Res. Solid Earth* **1996**, *101*, 21815–21828. https://doi.org/10.1029/96JB01308
50. Glazner, A.F.; Manley, C.R.; Marron, J.S.; et al. Fire or ice: Anticorrelation of volcanism and glaciation in California over the past 800,000 years. *Geophys. Res. Lett.* **1999**, *26*, 1759–1762. https://doi.org/10.1029/1999GL900333
51. McGuire, W.J.; Howarth, R.J.; Firth, C.R.; et al. Correlation between rate of sea-level change and frequency of explosive volcanism in the Mediterranean. *Nature* **1997**, *389*, 473–476. http://dx.doi.org/10.1038/38998
52. Watt, S.F.; Pyle, D.M.; Mather, T.A. The volcanic response to deglaciation: Evidence from glaciated arcs and a reassessment of global eruption records. *Earth-Sci. Rev.* **2013**, *122*, 77–102. https://doi.org/10.1016/j.earscirev.2013.03.007
53. Moran, S.C.; Zimbelman, D.R.; Malone, S.D. A model for the magmatic–hydrothermal system at Mount Rainier, Washington, from seismic and geochemical observations. *Bull. Volcanol.* **2000**, *61*, 425–436. http://dx.doi.org/10.1007/PL00008909
54. Hurst, T.; Smith, W. A Monte Carlo methodology for modelling ash-fall hazards. *J. Volcanol. Geotherm. Res.* **2004**, *138*, 393–403. http://dx.doi.org/10.1016/j.jvolgeores.2004.08.001
55. Fedotov, S.A.; Zharinov, N.A. On the eruptions, deformation, and seismicity of Klyuchevskoy Volcano, Kamchatka in 1986–2005 and the mechanisms of its activity. *J. Volcanol. Seismol.* **2007**, *1*, 71–97. https://doi.org/10.1134/S0742046307020017
56. Eibl, E.P.; Bean, C.J.; Einarsson, B.; et al. Seismic ground vibrations give advanced early-warning of subglacial floods. *Nat. Commun.* **2020**, *11*, 2504. https://doi.org/10.1038/s41467-020-15744-5
57. Hurwitz, S.; Lowenstern, J.B. Dynamics of the Yellowstone hydrothermal system. *Rev. Geophys.* **2014**, *52*, 375–411. https://doi.org/10.1002/2014RG000452
58. Satow, C.; Gudmundsson, A.; Gertisser, R.; et al. Eruptive activity of the Santorini Volcano controlled by sea-level rise and fall. *Nat. Geosci.* **2021**, *14*, 586–592. https://doi.org/10.1038/s41561-021-00783-4
59. Gahalaut, K.; Gahalaut, V.K.; Kayal, J.R. Poroelastic relaxation and aftershocks of the 2001 Bhuj earthquake, India. *Tectonophysics* **2008**, *460*, 76–82. https://doi.org/10.1016/j.tecto.2008.07.004
60. Kundu, B.; Legrand, D.; Gahalaut, K.; et al. The 2005 volcano-tectonic earthquake swarm in the Andaman Sea: Triggered by the 2004 great Sumatra–Andaman earthquake. *Tectonics* **2012**, *31*, TC5009. https://doi.org/10.1029/2012TC003138
61. Obara, K.; Kato, A. Connecting slow earthquakes to huge earthquakes. *Science* **2016**, *353*, 253–257. https://doi.org/10.1126/science.aaf1512
62. Parisio, F.; Vilarrasa, V.; Wang, W.; et al. The risks of long-term re-injection in supercritical geothermal systems. *Nat. Commun.* **2019**, *10*, 12146. https://doi.org/10.1038/s41467-019-12146-0
63. Schultz, R.; Skoumal, R.J.; Brudzinski, M.R.; et al. Hydraulic fracturing-induced seismicity. *Rev. Geophys.* **2020**, *58*, e2019RG000695. https://doi.org/10.1029/2019RG000695
64. Panda, D.; Kundu, B.; Gahalaut, V.K.; et al. Seasonal modulation of deep slow-slip and earthquakes on the Main Himalayan Thrust. *Nat. Commun.* **2018**, *9*, 1–8. https://doi.org/10.1038/s41467-018-06371-2
65. Schulz, W.H.; Kean, J.W.; Wang, G.; et al. Landslide movement in southwest Colorado triggered by atmospheric tides. *Nat. Geosci.* **2009**, *2*, 863–866. https://doi.org/10.1038/ngeo659
66. Matthews, A.J.; Barclay, J.; Johnstone, J.E. The fast response of volcano-seismic activity to intense precipitation: Triggering of primary volcanic activity by rainfall at Soufrière Hills Volcano, Montserrat. *J. Volcanol. Geotherm. Res.* **2009**, *184*, 405–415. https://doi.org/10.1016/j.jvolgeores.2009.05.010
67. Yamasato, H.; Kitagawa, S.; Komiya, M. Effect of rainfall on dacitic lava dome collapse at Unzen volcano, Japan. *Pap. Meteorol. Geophys.* **1998**, *48*, 73–78. https://doi.org/10.2467/mripapers.48.73
68. Violette, S.; De Marsily, G.; Carbonnel, J.P.; et al. Can rainfall trigger volcanic eruptions? A mechanical stress model of "Piton de la Fournaise," Reunion Island. *Terra Nova* **2001**, *13*, 18–24. https://doi.org/10.1046/j.1365-3121.2001.00297.x
69. Lesparre, N.; Boudin, F.; Champollion, C.; et al. New insights on fractures deformation from tiltmeter data measured inside the Fontaine de Vaucluse karst system. *Geophys. J. Int.* **2017**, *208*, 1389–1402. https://doi.org/10.1093/gji/ggw446
70. Banks, N.G.; Carvajal, C.; Mora, H.; et al. Deformation monitoring at Nevado del Ruiz, Colombia — October 1985–March 1988. *J. Volcanol. Geotherm. Res.* **1990**, *41*, 269–295. https://doi.org/10.1016/0377-0273(90)90092-T
71. Keir, D.; Ebinger, C.J.; Stuart, G.W.; et al. Strain accommodation by magmatism and faulting as rifting proceeds to breakup: Seismicity of the northern Ethiopian rift. *J. Geophys. Res. Solid Earth* **2006**, *111*, B05403. https://doi.org/10.1029/2005JB003748
72. Husen, S.; Taylor, R.; Smith, R.B.; et al. Changes in geyser eruption behavior and remotely triggered seismicity in Yellowstone National Park produced by the 2002 M 7.9 Denali earthquake. *Geology* **2004**, *32*, 537–540. https://doi.org/10.1130/G20381.1
73. Ogiso, M.; Matsubayashi, H.; Yamamoto, T. Descent of tremor source locations before the 2014 phreatic eruption of Ontake volcano, Japan. *Earth Planets Space* **2015**, *67*, 1–12. https://doi.org/10.1186/s40623-015-0376-y
74. Lowrie, W. *A Student's Guide to Geophysical Equations*; Cambridge University Press: Cambridge, London, UK, 2011.
75. Matsumoto, K.; Sato, T.; Takanezawa, T.; et al. GOTIC2: A program for computation of oceanic tidal loading effect. *J. Geod. Soc. Jpn.* **2001**, *47*, 243–248. https://doi.org/10.11311/jgeography.110.247
76. Sahoo, S.; Senapati, B.; Panda, D.; et al. Tidal triggering of seismic swarm associated with hydrothermal circulation at Blanco Ridge transform fault zone, NE Pacific. *Phys. Earth Planet. Inter.* **2024**, *356*, 107259. https://doi.org/10.1016/j.pepi.2024.107259
77. Bhatnagar, T.; Tolstoy, M.; Waldhauser, F. Influence of fortnightly tides on earthquake triggering at the East Pacific Rise at $9°50'$N. *J. Geophys. Res. Solid Earth* **2016**, *121*, 1262–1279. https://doi.org/10.1002/2015JB012365
78. Varga, P.; Grafarend, E. Influence of tidal forces on triggering of seismic events. In *Geodynamics and Earth Tides Observations*; Springer: Cham, Switzerland, 2019; pp 55–63. http://dx.doi.org/10.1007/978-3-319-96277-1_6
79. Agnew, D. *SPOTL: Some Programs for Ocean-Tide Loading*. SIO Technical Report; Scripps Institution of Oceanography, University of California: La Jolla, CA, USA, 2012.
80. Ray, R.D. A global ocean tide model from TOPEX/POSEIDON altimetry: GOT99.2. NASA Tech. Memo.; Goddard Space Flight Center: Greenbelt, MD, USA, 1999.
81. Mogi, K. Relations between the eruptions of various volcanoes and the deformations of the ground surfaces around them. *Bull. Earthquake Res. Inst.* **1958**, *36*, 99–134.
82. Okada, Y. Surface deformation due to shear and tensile faults in a half-space. *Bull. Seismol. Soc. Am.* **1985**, *75*, 1135–1154. https://doi.org/10.1785/BSSA0750041135
83. Dzurisin, D.; Lisowski, M. Analytical volcano deformation source models. In *Volcano Deformation: Geodetic Monitoring Techniques*; Springer: Berlin, Germany, 2007; pp 279–304. http://dx.doi.org/10.1007/978-3-540-49302-0_8

84. Battaglia, M.; Cervelli, P.F.; Murray, J.R. dMODELS: A MATLAB software package for modeling crustal deformation near active faults and volcanic centers. *J. Volcanol. Geotherm. Res.* **2013**, *254*, 1–4. https://doi.org/10.1016/j.jvolgeores.2012.12.018

85. Dvorak, J.J.; Dzurisin, D. Volcano geodesy: The search for magma reservoirs and the formation of eruptive vents. *Rev. Geophys.* **1997**, *35*, 343–384. https://doi.org/10.1029/97RG00070

86. Wicks, C.; Thatcher, W.; Dzurisin, D. Migration of fluids beneath Yellowstone caldera inferred from satellite radar interferometry. *Science* **1998**, *282*, 458–462. https://doi.org/10.1126/science.282.5388.458

87. Ziv, A.; Rubin, A.M. Static stress transfer and earthquake triggering: No lower threshold in sight? *J. Geophys. Res.* **2000**, *105*, 13631–13642. https://doi.org/10.1029/2000jb900081

88. Scholz, C.H.; Tan, Y.J.; Albino, F. The mechanism of tidal triggering of earthquakes at mid-ocean ridges. *Nat. Commun.* **2019**, *10*, 2526. https://doi.org/10.1038/s41467-019-10308-5